ČERVENKA CONSULTING

Červenka Consulting s.r.o.
Na Hřebenkách 55
150 00 Prague
Czech Republic
Phone: +420 220 610 018
E-mail: cervenka@cervenka.cz
Web: https://www.cervenka.cz

GREEN CONCRETE PRE-CAST ELEMENTS DESIGN AND OPTIMIZATION

Project Result TM04000013-V5

Written by

Jan Červenka

Zdeněk Bittnar

Ondřej Zobal

Kočková Eliška

Petr Havlásek

Luboš Řehounek

Version 5.0

Prague, December 2025

Contents

Executive Summary 3
1 Introduction 4
2 Technology of New-MRCS Systems 5
2.1 New-MRCS System Description 6
2.2 Experimental Results for MRCS Connections 7
2.3 ATENA Modelling (CC) 8
2.4 OOFEM Modelling (CTU) 9
3 Concrete Material Properties (CTU) 13
4 Design by Numerical Simulation 17
4.1 Nonlinear Modelling 17
4.2 Concrete Material Model with Time Dependent Properties 18
4.3 Safety Formats for Design by Numerical Simulation 21
4.3.1 Model Uncertainties and Safety Factors 21
4.4 Modelling and Design of Optimized Construction Sequence for Green Concrete Materials 22
5 Example of Application (CC) 24
5.1 Example of Column-Beam Connection Modelling and Design 24
5.1.1 Step 1: Estimation of time history of stress development in the critical concrete elements. 28
5.1.2 Step 2: Map stress history development into the green concrete database of material maturity curves. 28
5.1.3 Step 3: Select suitable material and optimize the construction sequence. 29
5.1.4 Step 4: Verify the selected material and construction sequence by numerical simulation in ATENA-Green Concrete Module. 31
5.2 Example of Composite Frame Modelling and Design 34
5.2.1 Step 1: Estimation of time history of stress development in the critical concrete elements. 37
5.2.2 Step 2: Map stress history development into the green concrete database of material maturity curves. 37
5.2.3 Step 3: Select suitable material and optimize the construction sequence. 38
5.2.4 Step 4: Verify the selected material and construction sequence by numerical simulation in ATENA-Green Concrete Module. 39
6 Conclusion 44
7 References 45

Executive Summary

This document presents the **Green Concrete Pre-Cast Elements Design and Optimization Methodology**, developed as the project result **TM04000013-V5** within the bilateral research project **CeSTaR-3**, funded by the Technology Agency of the Czech Republic under the **DELTA 2 Programme**. The result provides a **practical design and optimization framework** for precast concrete structural elements made of **green concrete with a high replacement rate of Portland cement by supplementary cementitious materials (SCMs)**.

The methodology addresses a key challenge associated with green concrete technologies: the **time-dependent development of mechanical properties** and its interaction with **manufacturing, installation, and loading sequences** typical for precast construction. While green concrete enables significant reductions in CO_2 emissions, its slower strength development requires a design approach that explicitly accounts for different construction stages rather than relying solely on conservative early-age material assumptions.

The proposed methodology combines:

- **experimentally validated material data** obtained within the CeSTaR-3 project and compiled in the experimental database of green concrete materials (**project result TM04000013-V6**), and
- **advanced nonlinear numerical simulation** using the ATENA software environment extended by the CeSTaR-3 Green Concrete Module (**project result TM04000013-V2**).

Based on these inputs, the methodology defines a **structured design workflow** for precast green-concrete elements, including:

- selection of suitable concrete mixtures with respect to required performance at different construction stages,
- evaluation of strength development and confinement effects,
- optimization of construction and installation sequences,
- verification of structural performance using nonlinear numerical simulation and appropriate safety formats.

The document provides **design principles, recommended procedures, and example applications** illustrating how the methodology can be applied in engineering practice. The focus is placed on **design optimization**, enabling more efficient use of materials while maintaining structural safety and reliability. The methodology is intended for **structural engineers, designers of precast systems, and researchers** involved in the application of sustainable concrete technologies.

By linking experimental research, numerical simulation, and practical design guidance, the Green Concrete Pre-Cast Elements Design and Optimization Methodology supports the **practical adoption of low-carbon concrete technologies** in precast construction. The result represents a key applied outcome of the CeSTaR-3 project, contributing to more sustainable and resource-efficient construction practices through informed design and optimization.

1 Introduction

The increasing demand for **sustainable construction practices** has led to the development and application of **green concrete technologies**, in which a significant portion of Portland cement is replaced by supplementary cementitious materials (SCMs). While such materials offer substantial environmental benefits, their use introduces **time-dependent material behaviour** that differs from conventional concrete, particularly with respect to early-age strength development and stiffness evolution.

These effects are especially relevant in **precast concrete construction**, where structural elements are manufactured, transported, assembled, and loaded in a sequence of well-defined construction stages. Conventional design approaches typically rely on conservative assumptions regarding early-age material properties, which may lead to inefficient use of materials, overly restrictive construction schedules, or unnecessary safety margins when applied to green concrete systems.

The CeSTaR-3 project addresses this challenge by integrating **experimental research**, **advanced numerical modelling**, and **design-oriented methodologies**. Within this framework, the present document introduces a **Green Concrete Pre-Cast Elements Design and Optimization Methodology** (project result TM04000013-V5), intended to support informed design decisions that explicitly account for the **interaction between material strength development and construction sequence**.

The methodology builds on:

- experimentally validated material data for green concrete mixtures obtained within the CeSTaR-3 project and compiled in the experimental database (**TM04000013-V6**), and
- nonlinear numerical simulation using the ATENA software environment extended by the CeSTaR-3 Green Concrete Module (**TM04000013-V2**).

By combining these inputs, the methodology provides a **structured design framework** for precast green-concrete elements, enabling:

- selection of appropriate concrete mixtures with respect to required performance at different stages of construction,
- assessment of confinement and system effects typical for precast elements,
- optimization of manufacturing, installation, and loading sequences,
- verification of structural safety using nonlinear analysis and suitable safety formats.

This document is intended as a **methodological guideline** rather than a software manual or experimental report. It focuses on **design principles, recommended procedures, and decision logic** that can be applied in engineering practice. Detailed descriptions of experimental testing and software implementation are provided in separate CeSTaR-3 project results and are referenced where necessary.

The methodology is applicable to a broad class of **precast reinforced and prestressed concrete elements**, particularly where time-dependent material behavior and staged construction play a significant role. Its primary users are **structural engineers, designers of precast systems, and researchers** involved in the development and application of sustainable concrete technologies.

2 Technology of New-MRCS Systems

The technology of **New-MRCS structural systems** represents an advanced development of conventional reinforced concrete and composite structural solutions, aimed at achieving **higher structural efficiency and reduced environmental impact**. The system combines **prefabricated reinforced concrete columns** with **steel beams**, while incorporating material and technological innovations that enable a substantial reduction in CO_2 emissions compared to traditional construction approaches.

The new-MRCS system is a green upgrade to the previous new-RCS technology developed in Taiwan, which started in 2019. Thus, the new-MRCS project will use:

1. Optimized prefabricated construction with high-strength and green materials (New)

2. Multi-spiral Reinforced Concrete columns and Steel beams (MRCS)

3. Effective use of Supplementary Cementitious Materials (SCM) based on principles of performance-based design.

A key component of the New-MRCS technology is the use of **green concrete with a high replacement rate of Portland cement by supplementary cementitious materials (SCMs)**. Such concrete mixtures significantly reduce the carbon footprint of structural elements; however, they exhibit **time-dependent strength development** that differs from conventional concrete. This behavior has a direct influence on the design, manufacturing, and assembly of prefabricated elements and therefore must be explicitly considered in the structural design process.

The New-MRCS system further exploits **prefabrication-oriented construction principles**, where columns and other structural components are produced off-site and assembled on-site in a staged construction sequence. This approach improves construction quality and productivity while allowing flexibility in scheduling and load application. In particular, the ability to consider **later-age concrete strength** (e.g. 56-day or 90-day strength instead of the standard 28-day strength) enables the effective use of green concrete with slow strength development, without compromising structural safety.

An additional technological innovation of the New-MRCS system is the application of **multi-spiral transverse reinforcement** in concrete columns. Compared to conventional rectilinear ties, multi-spiral reinforcement provides improved confinement of the concrete core, enhanced ductility, and a more efficient use of reinforcement steel. This reinforcement layout is well suited for prefabrication and automated production, contributing further to material savings and environmental benefits.

The development and validation of the New-MRCS technology are based on a **synergistic combination of experimental research and numerical modelling**. Experimental investigations provide essential insight into the behavior of green concrete under different loading and confinement conditions, while advanced numerical models enable the evaluation of structural response at both element and system levels. These modelling tools support the assessment of construction stages, load redistribution, and safety verification, which are critical aspects of New-RCS system design.

Within the CeSTaR-3 project, the New-MRCS technology serves as a **reference application domain** for the proposed design and optimization methodology. It demonstrates how green concrete materials, innovative reinforcement concepts, and staged construction can be integrated into a coherent structural system. The New-RCS system thus provides a practical framework for applying the methodology presented in this document and illustrates its relevance for modern, sustainable prefabricated construction.

2.1 New-MRCS System Description

The New-MRCS (New Multi-spiral Reinforced Concrete–Steel) system is a **prefabricated hybrid structural system** combining reinforced concrete columns with steel beams, developed to improve structural efficiency and reduce environmental impact. The system extends the conventional MRCS/RCS concept by integrating **green concrete with a high content of supplementary cementitious materials (SCMs)** and advanced reinforcement layouts suitable for prefabricated construction.

A key characteristic of the New-MRCS system is the use of **prefabricated concrete columns** manufactured with green concrete mixtures and assembled on site together with steel beams in a staged construction process. This approach enables efficient production, flexible construction sequencing, and controlled application of loads during erection.

Concrete columns in the New-MRCS system employ **multi-spiral transverse reinforcement**, providing enhanced confinement of the concrete core, improved ductility, and a more efficient use of reinforcement steel compared to conventional rectilinear ties. The multi-spiral reinforcement layout is well suited for automated prefabrication and repeatable production.

The development of MRCS and subsequently New-MRCS structural systems builds on earlier reinforced concrete–steel (RCS) concepts, which have been successfully applied in practice, including real building projects constructed by industrial partners in Taiwan. Initial new-RCS applications employed conventional rectilinear transverse reinforcement in concrete columns and demonstrated the feasibility of prefabricated concrete columns combined with steel beams in multi-storey buildings. Experience gained during the construction of these buildings, together with close collaboration between researchers and industry, revealed the need for further research focusing on structural behaviour under **high axial loads** and on improving material efficiency. This led to the introduction of **multi-spiral transverse reinforcement** to enhance confinement and ductility of concrete columns, as well as to the integration of **green concrete with higher SCM replacement** (see Fig. 1). The New-MRCS system represents a continuation and green upgrade of the earlier new-RCS concept, combining prefabrication, multi-spiral reinforcement, and performance-based use of sustainable concrete materials.

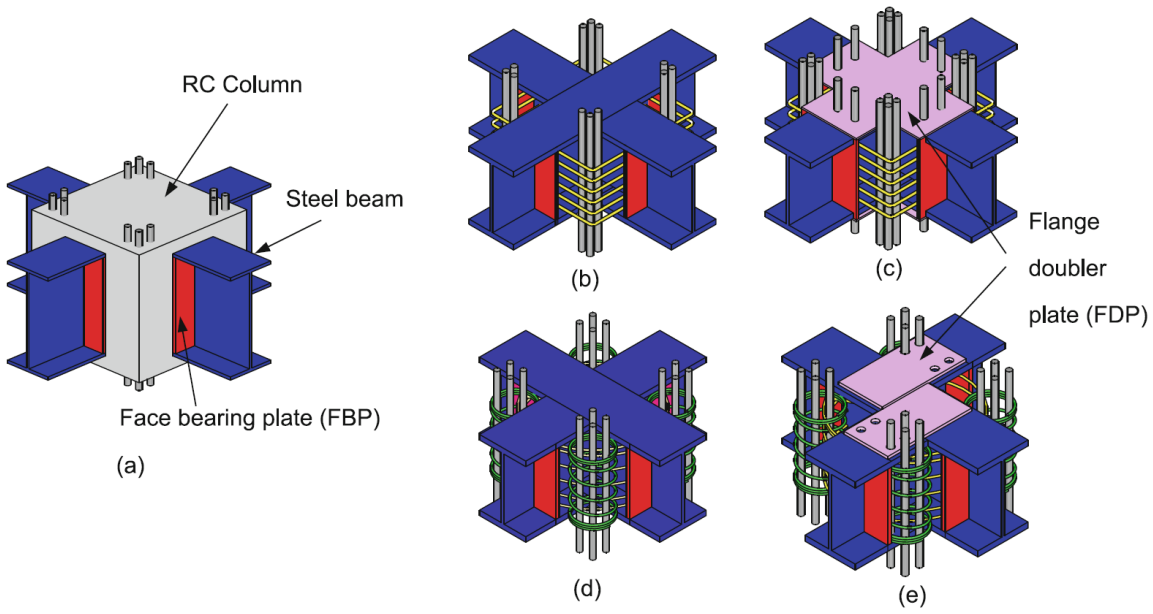

Fig. 1: a) Conventional through-beam type RCS joint; b) Conventional joint with rectilinear ties; c) joint with realistic longitudinal reinforcement ratio; d) joint with five-spiral transverse reinforcement; e) eccentric joint.

2.2 Experimental Results for MRCS Connections

An extensive experimental program was carried out within the by the **Taiwanese project partners**, providing the fundamental experimental background for the development of the New-MRCS structural system. The experimental activities were designed to investigate the structural behavior of key system components and materials relevant to MRCS and New-MRCS applications, with a focus on conditions representative of practical building structures [33][34][35][46].

The experimental investigations addressed the behavior of **reinforced concrete elements and connections**, including the influence of **axial load level, confinement, reinforcement layout, and material properties**. Particular attention was devoted to structural configurations typical for MRCS systems, such as concrete columns interacting with steel beams and connection regions subjected to combined loading effects.

A substantial part of the experimental program was dedicated to the study of **concrete with increased replacement of Portland cement by supplementary cementitious materials (SCMs)**. These tests provided essential information on the **time-dependent development of mechanical properties**, which is a key characteristic of green concrete and a governing factor for prefabricated construction and staged loading scenarios.

The results of the experimental program form the **empirical basis for the design assumptions and modelling approaches** adopted in the New-MRCS methodology. Rather than being used directly for design, the experimental data support the development of material models, validation of numerical simulations, and formulation of performance-based design principles. Detailed descriptions of the experimental setups, results, and interpretations are documented in project reports and publications produced by the Taiwanese partners and are referenced where appropriate.

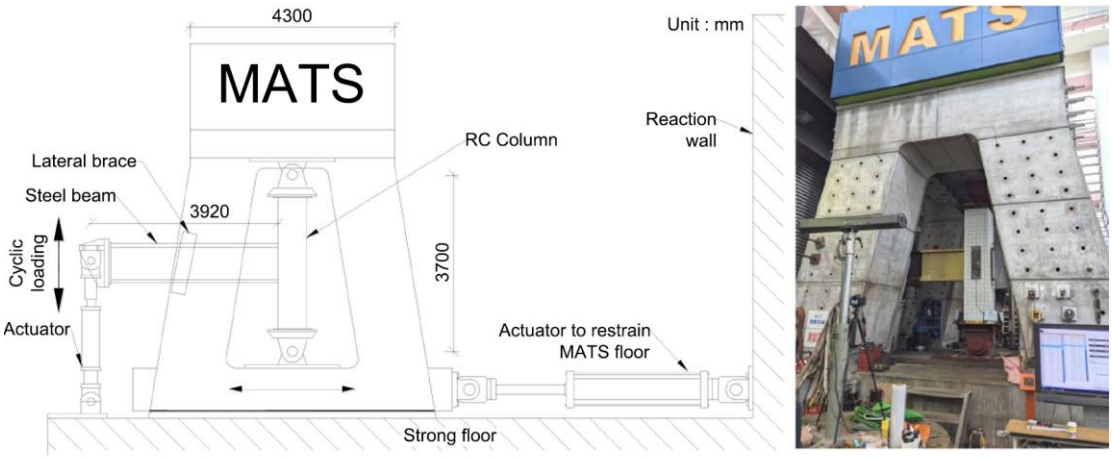

Fig. 2: (a) View of the typical experimental setup, and (b) photo of the unique MATS experimental machine used for the experiments [34].

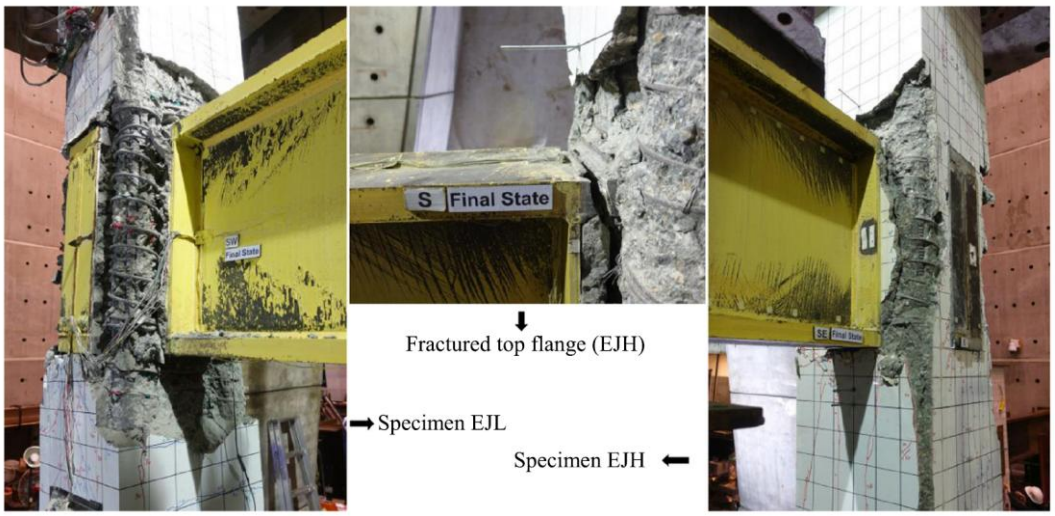

Fig. 3: Typical view of the damaged RCS specimens after the test [34].

2.3 ATENA Modelling

The experiments performed by Joju [32],[34] have been used for the validation of the numerical model in ATENA software. ATENA model takes into account all important elements of the New-MRCS connection (see Fig. 4). The model was developed using the new ATENA module developed during CeSTaR-2 project [20]. This new module allows the parametric definition and cycling as well as dynamic modelling of the these specialized pre-cast connections.

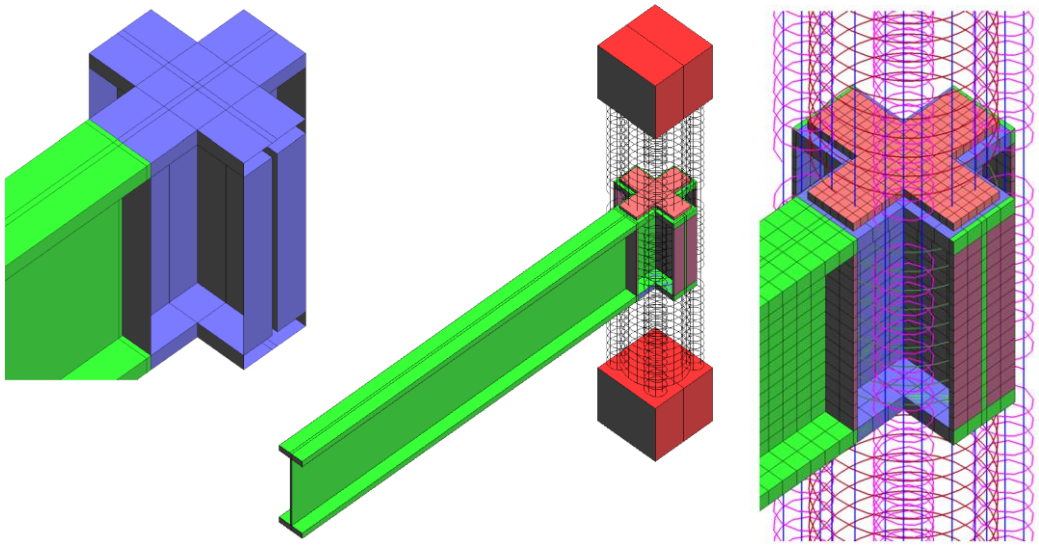

Fig. 4: Details of the numerical model in ATENA software developed using the new CeSTaR-3 module.

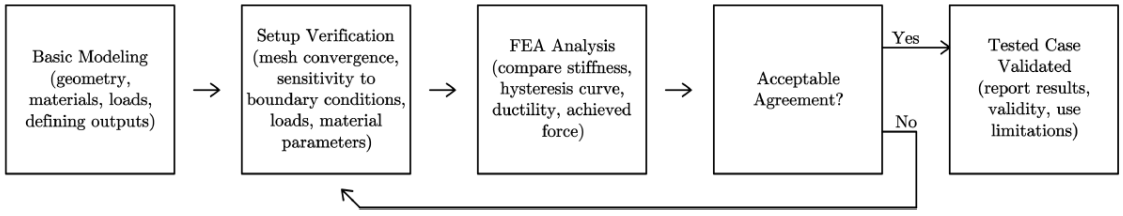

Fig. 5: Schema of the workflow of the validation of the New-MRCS connection model.

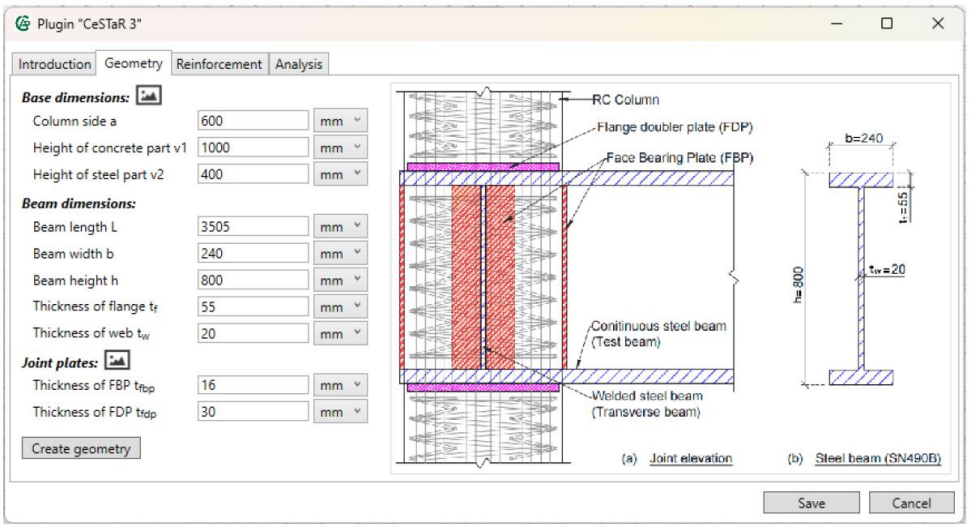

Fig. 6: Parametric generation and modelling of the New-MRCS connections [20].

The validation process as well as the new parametric and scripting options in the new ATENA module are described in the software documentation [20] and the publication [42]. The validation workflow is shown in Fig. 5. Very good agreement was obtained in modelling the cycling behavior of the pre-cast connections as shown in Fig. 7.

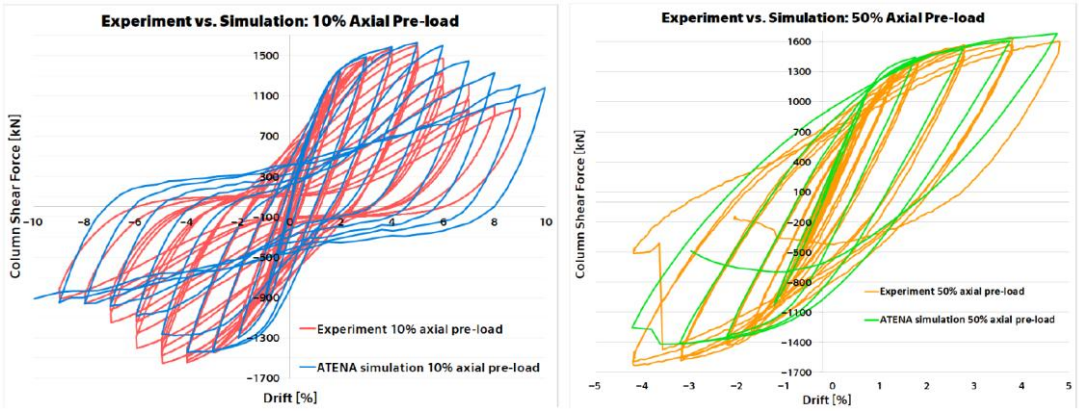

Fig. 7: Comparison of the validated cycling responses of New-MRCS connections with different levels of axial loads.

2.4 OOFEM Modelling

The finite element package OOFEM [40] is an open-source solver developed primarily at the Faculty of Civil Engineering, Czech Technical University in Prague. One of its key advantages is an extensive library of state-of-the-art material models for concrete, including both time-dependent and highly nonlinear behavior typical of extreme loading conditions.

The most suitable material model for simulating short-term concrete response under various stress states is the second generation of the Damage-Plastic Model for Concrete Failure, CDPM2 [28], developed and implemented by Grassl and coworkers. This model enables one to capture of all important phenomena salient for confined concrete, i.e., the increase in strength and ductility under multiaxial compressive stress states, while simultaneously capturing tensile cracking, which is important when modeling concentrated loading such as in the case of New MSRC joints.

Although this material model is not inherently time-dependent, the time-dependence of evolving material properties can be easily defined by modifying the material parameters of the constitutive

model. Some of these parameters are directly associated with the fundamental properties of concrete and/or concrete maturity via empirical expressions from design codes, such as the *fib* Model Code 2020 [26].

The CDPM2 model is based on plasticity with isotropic hardening and non-associated flow, combined with a scalar damage model where damage is driven by plastic flow and elastic strain. The yield condition is formulated in the effective stress space and depends on all three stress invariants. The yield function adopts the shape of the deviatoric section proposed by Willam and Warnke and further extends the failure surface suggested by Menétrey and Willam.

The flow rule is derived from a plastic potential that depends only on the hydrostatic stress and the second deviatoric invariant, which improves implementation efficiency and model robustness. The model operates with effective stress, which is computed using the plastic part of the model. Two independent scalar damage variables for tension and compression are used, enabling the transition from effective to nominal stress.

To prevent mesh-dependent results, the model can be regularized by, for example, a nonlocal approach; however, owing to the additional parameters involved in that technique and its high computational demands, regularization is performed here by adjusting a parameter that controls the evolution of tensile damage according to the element size—a method often referred to as the crack-band approach of Bažant.

A crucial aspect of model calibration is prioritizing which phenomena are most critical for the analysis of a specific structural detail: the increase in strength due to confinement or tensile cracking. In structural joints, behavior under confinement is typically the governing factor. The model is formulated such that the yield surface of the plastic component depends on both the uniaxial tensile and compressive strengths. While this may seem like a subtle detail to the user, it can have crucial consequences on the predicted behavior.

Experience indicates that even when the exact tensile strength is known from experimental data or estimated from design codes (based on compressive strength), the most effective strategy is to set the tensile strength to 10% of the compressive strength (f_t = 0.1 f_c). Although this value may overestimate the actual tensile strength or appear physically unrealistic, it ensures the most accurate response under multiaxial compressive stress states. Adhering to the actual (lower) tensile strength often leads the model to significantly overestimate the confined response. The difference between two approaches is illustrated in Fig. 8.

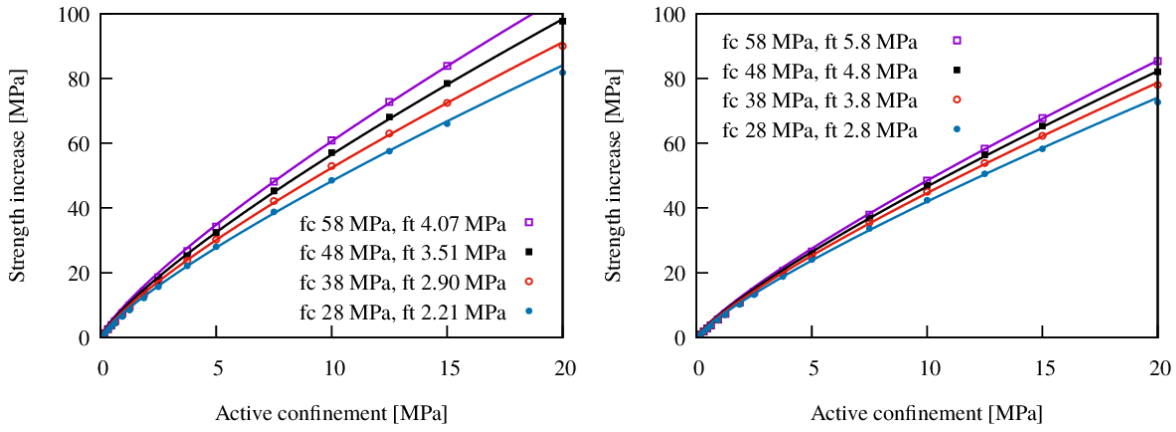

Fig. 8: Increase in strength produced by active confinement as predicted by CDPM2 with ft according to (left) *fib* MC 2010, (b) ft = 0.1 fc. FEM results marked by points are approximated by simplified power expressions shown by lines.

The remaining model parameters can be kept at their default values or identified through a more complex approach using the [45] within the theoretical framework developed in [36].

Performance of the CDPM2 material model in FE solver OOFEM is demonstrated on two examples shown in Fig. 9 and Fig. 10 adapted from an extensive study on applicability of CDPM2 to confined concrete presented in [30]. In these examples, concrete was modeled with a single finite element (and the stress-state was assumed to be homogeneous, Fig. 11)

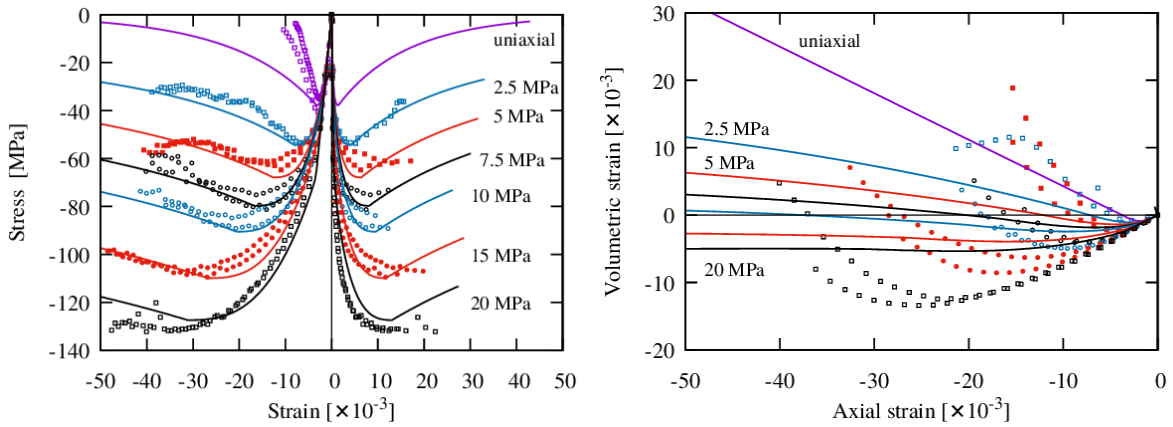

Fig. 9: Comparison of FEM simulation with compression tests on actively confined concrete cylinders by Li [37], (left) axial stress versus axial and lateral strains, (right) dependence of the volumetric strain on axial strain.

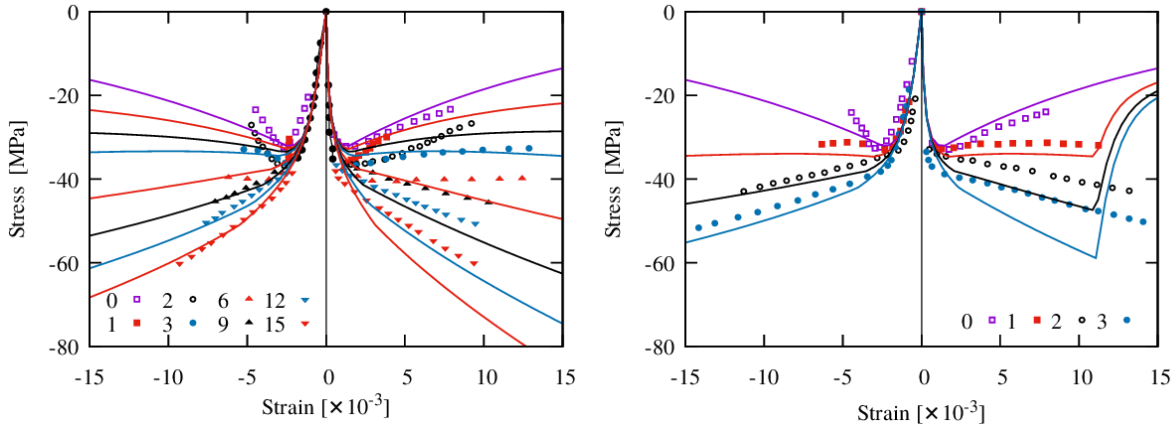

Fig. 10: Comparison of FEM simulation with compression tests on passively confined concrete cylinders by Harries [29], passive confinement imposed by (left) glass and (b) carbon wrapping. Stronger black points in (right) denote the loading path common for all confined specimens.

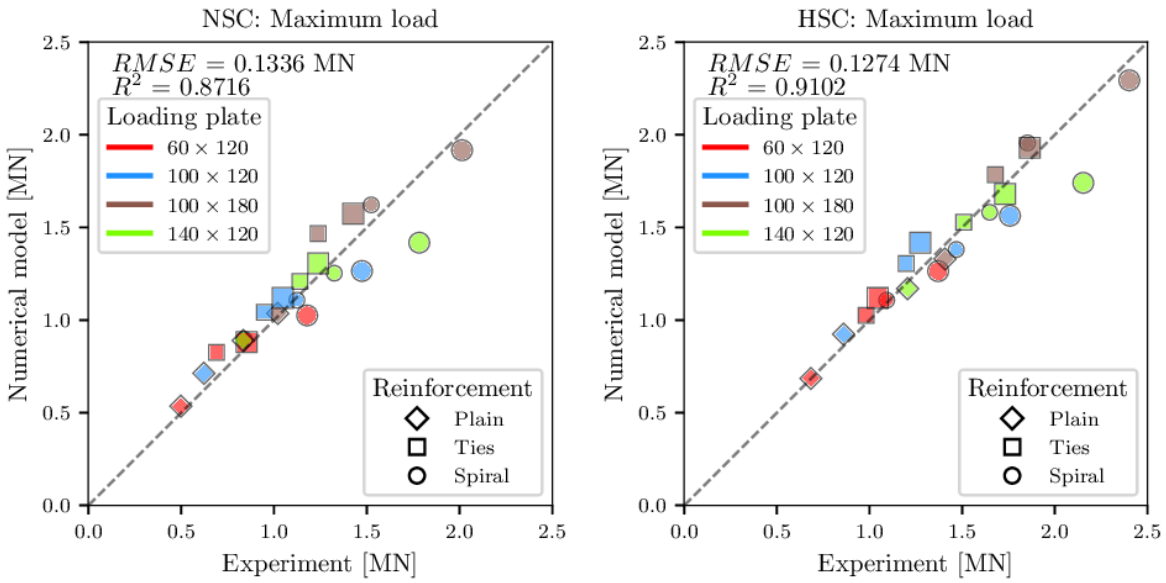

Fig. 11: Comparison of FEM simulations with bearing strength experimental results from the CeSTaR 3 project. Simulations were performed using an increased tensile strength (ft = 0.1 fc) to mitigate the excessive confinement-induced strength increase and minimize the discrepancy between numerical and experimental results. The left figure corresponds to normal-strength concrete (f_c = 45.8 MPa), while the right figure corresponds to high-strength concrete (f_c = 63.3 MPa).

3 Concrete Material Properties

The material properties of concrete play a decisive role in the design and optimization methodology presented in this document, particularly when **green concrete with an increased content of supplementary cementitious materials (SCMs)** is used. Unlike conventional concrete, green concrete typically exhibits a **pronounced time-dependent development of mechanical properties**, which directly influences structural response during manufacturing, transportation, erection, and early service stages.

Within the proposed methodology, concrete material properties are not treated as fixed values corresponding to a single reference age, but as **time-evolving parameters** that reflect the actual maturity and curing conditions of the material. This approach is essential for prefabricated and staged construction systems, where structural elements are subjected to loading at different ages and under varying boundary conditions.

The material characteristics considered include the **development of compressive and tensile strength, stiffness, fracture-related parameters, and confinement effects** relevant for reinforced and confined concrete elements. These properties form the basis for assessing resistance at different construction stages and for evaluating utilization levels in the optimization of construction sequences.

The definitions and assumptions adopted in this section provide the **material input framework** for the numerical design and optimization procedures described in subsequent sections. Detailed experimental characterization and calibration of material parameters are documented separately in the experimental database developed within the CeSTaR-3 project, while this section focuses on the **methodological use of material properties in design and numerical simulation**.

3.1 Preparation

Preparation consists of designing the composition of the concrete mixture and determining the degree of prestressing, which is given by the used rings (number, material, wall thickness, placement). Next, it is necessary to determine the number and size of test specimens to be produced. For one measurement (1 set: 1 mixture, 1 age) 6 cylindrical specimens are typically required – 3 basic specimens (these specimens are used to determine the basic strength of the produced concrete) and 3 specimens with reinforcement.

3.2 Production of specimens

There are two options for production of specimens with rings. The first option is when the outer diameter of the ring corresponds to the inner diameter of the mold. In this case, plastic spacer rings of the same diameter and thickness are placed between the individual rings and gradually inserted directly into the mold.

The second option is more versatile, but slightly more demanding, as it requires a larger number of unique parts (called inserts) that must be prepared and manufactured in advance (according to the parameters of the rings). The individual parts are assembled together and the combination with inserted rings, form a complete modular system, resulting in the creation of a "custom mold within a standard mold". All parts can be manufactured using 3D printing, making it a modern and cost-effective solution that does not require any special machinery. The main advantage of this solution is its complete versatility in the choice of any ring dimensions and the associated maintenance of the standard 2:1 ratio of diameter to height of the test specimen when using a standard steel mold. A detailed description of the above is available in the Utility Model Application Document, which includes a description of the technical solution and documentation

(drawings) submitted to the Industrial Property Office of the Czech Republic – "Úřad průmyslového vlastnictví – ÚPV", which issued the registration certificate [45]. This certificate proves our rights to the protected technical solution.

Fig. 12: Demonstration of the principle of assembling individual parts (inserts) and aluminum rings (left). The individual layers are made up of two parts with locks so that they can be removed during demolding. The result is a "custom mold inserted into a standard mold" (right).

After removing the specimens from the mold (demolding), the plastic spacer rings (variant 1) or individual parts of the modular system (variant 2) are removed. In both cases, the result is a test specimen with rings on its body. To finish the specimen and achieve plane parallelism (parallelism of opposite surfaces), its upper side is ground in a special device.

After production, the specimens are stored in a box with a water-saturated environment, not directly in water, until testing.

3.3 Testing and measurement

If the non-contact optical method of digital image correlation is used, it is first necessary to apply a random black-and-white structure, known as a speckle pattern, to the surface of the samples. First, a matte white base coat is applied. Then, fine black dots are created (typically using a spray in the case of concrete samples).

Next, it is necessary to adjust the optical system – the cameras (for cylindrical bodies, 3D measurement using a stereoscopic system of two cameras is recommended) and lighting (intensity)—so that there are no false reflections, which the software would evaluate incorrectly or not evaluate at all. The final step is calibration—using a calibration plate, the parameters and mutual position of the cameras in space are defined.

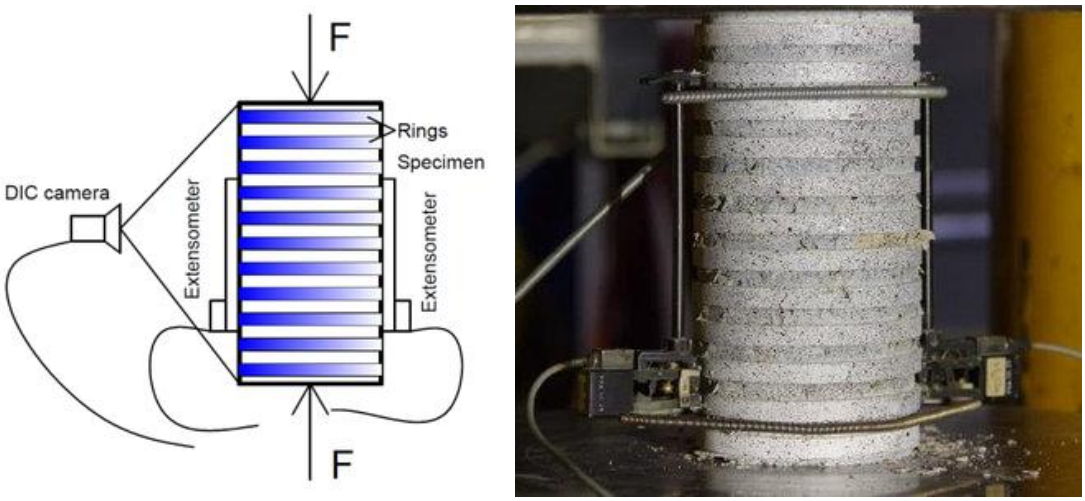

Fig. 13: Concrete specimen strengthened by external reinforcement in the shape of rings. Principle setup scheme of the measurement of deformation (left) and specimen with attached extensometers and also with sprayed pattern for DIC after completion of the compressive test (right).

Before the actual testing, the specimen is measured – weight, diameter, height, and in the case of specimens with rings, also the height of the individual rings and their placement on the body. This is followed by the insertion and positioning of the test specimen into the hydraulic press. In the case of deformation measurements using extensometers (if the testing machine is equipped with them), they are attached using springs at this moment.

3.4 Data processing

The basic measured data includes time, force, and position of the hydraulic cylinder or crossbar (depending on the design of the loading machine), or extensometers. The recording of this data is controlled by the machine's control unit and is almost always available in csv or another text format. In the case of DIC measurement, the situation is much more complicated. At the beginning, a reference image of the body in an unloaded state is taken. Cameras scanning the surface at defined intervals throughout the test create a series of images. To obtain data from these images, digital processing (correlation) is necessary. The software divides the reference image into small square areas called facets (subsets). The algorithm searches for these specific facets in each image (of the deforming body) based on the mathematical correspondence of gray-scale values. The result is the calculation of a displacement vector for each facet. From the displacement of the facets, the software calculates the field of deformations or displacements. The results are visualized in the form of color maps directly on the 3D model of the body.

However, it is important to note that this post-processing and analysis is very time-consuming, as it is performed for each recorded image. This can involve a very large number and volume of images. It is usually a repetitive process, because for successful analysis it is first necessary to find the ideal settings for many parameters—facet size, mesh overlap, but often also manual searching, adding or removing starting points, which must be in the same logical place on each camera image (despite their different views). This is where automatic detection in 3D imaging often fails, and it is necessary to check the entire series of images. A serious complication is the loss of parts of the pattern, typically due to damage to the object or its parts, which makes it impossible to perform the calculation.

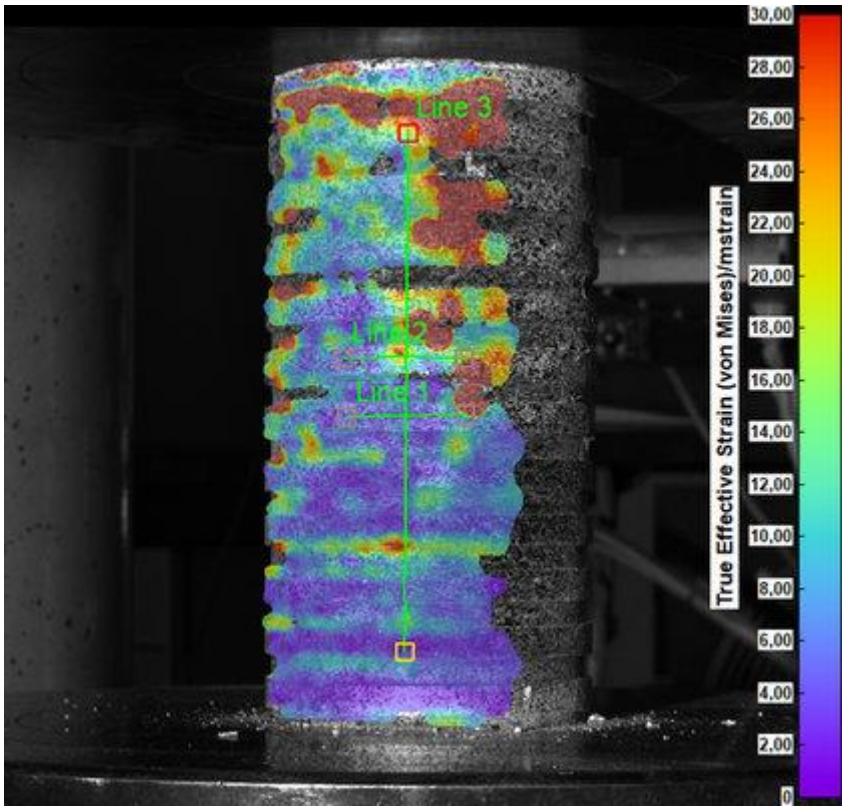

Fig. 14: Processing of measurements using DIC, where the result of data post-processing is visualized (e.g., field of deformations) on the body of the test specimen. Line 1 and Line 2 represent a virtual strain gauge located on the middle aluminum rings, Line 3 replaces the extensometer in the axis of uniaxial loading.

When performed correctly, DIC post-processing offers a wide range of possibilities for obtaining various data at any location on the body. Classic tasks include tracking the trajectory of points or user-defined virtual strain gauges. In our case, for example, placed on individual rings (i.e., in the transverse direction) or replacing contact extensometers (i.e., in the direction of uniaxial loading). Data can be exported as videos, images, and, of course, as numerical data for further use, e.g., for comparison with numerical models.

3.5 Effect of concrete specimens with confinement

With increasing age of the test specimens, an increase in strength can be expected, both in the case of basic specimens and in the case of specimens with confinement. The loading rate of the cylinders is the same in both cases.

Depending on the quality of the concrete mix, the measurement of the post-tensioning properties of clamped specimens depends on the relationship between the compressive strength of the concrete and the tensile strength of the clamping material. For example, lower-quality concrete will cause less brittle behavior in the post-tensioning phase of testing and vice versa.

4 Design by Numerical Simulation

Design by numerical simulation forms a central component of the proposed methodology for **New-MRCS structures incorporating green concrete with increased SCM content**. The purpose of numerical simulation within this methodology is not to replace standard design procedures, but to **support informed design and optimization decisions** in situations where time-dependent material behavior and staged construction significantly influence structural response.

The use of green concrete in prefabricated MRCS systems introduces design challenges related to **nonlinear behavior, confinement effects, and the evolution of material properties over time**. These aspects cannot be adequately addressed using simplified linear models or design checks based solely on a single reference age of concrete. Numerical simulation therefore, provides a rational framework for evaluating structural response during different construction and loading stages and for verifying the suitability of selected materials and construction sequences.

Within the proposed methodology, numerical simulation is applied in a **structured and targeted manner**, focusing on critical structural elements, connection regions, and construction phases. The simulation results are used to assess stress development, utilization levels, and damage indicators, and to guide the selection and optimization of concrete materials and construction procedures. The modelling approach is based on nonlinear finite element analysis and is consistent with performance-based design principles.

The detailed modelling assumptions, material representations, and safety formats adopted for design by numerical simulation are described in the following subsections. Together, they provide a practical and transparent framework for applying numerical simulation as a design and optimization tool within the New-MRCS methodology.

4.1 Nonlinear Modelling

The original publications on the finite element method, which is the main method used for nonlinear simulation, are due to J. Argyris (1954), M.J. Turner and R.W.Clough (1956), and O.C. Zienkiewicz (1967). It became the most significant tool for structural analysis and a basis of computer codes for solutions of engineering problems. A displacement-based version of the finite element method is the most popular version for the engineering applications and is used in this report.

The exact solution of the continuum problem is approximated by a solution of the set of linear equations for discrete number of nodal displacements. This discretization is illustrated in Fig. 15, where three solution levels are recognized, namely *structure* (describing the engineering task to be solved), *finite element* (defining an approximation by the finite element mesh), and *material* (defining a non-linear behavior). A nonlinear response (due to material behavior or geometry) is solved by an iterative Newton-Raphson method. The solution is illustrated in Fig. 15 and is described by the following set of matrix equations:

$$K_{n,i}\,\Delta U_{n,i} = P_n - R_{n,i} \tag{1}$$

$$K_{n,i} = \sum_{j=1}^{m} k_j,\ R_{n,i} = \sum_{j=1}^{m} r_j\ ,\ U_{n+1,i} = U_{n,i} + \Delta U_{n,i} \tag{2}$$

In this: K_i – stiffness matrix of the structure at the load step *n* and iteration i, ΔU_i – vector of displacement increments, $U_{n,i}$ – vector of total displacements of the structure in step n and iteration i, P_n – vector of total nodal forces at the load step *n*, $R_{n,i}$ – vector of resisting nodal forces, k_j – element stiffness matrix, r_j – vector of resisting element nodal forces. The number of rows in the matrix Equation (1) corresponds to the number of nodal displacements in the structure. Eq. (2) represents the assembly of the global stiffness matrix, nodal forces and nodal displacements as a summation from local element entities, where m is the number of finite elements. It should

be noted that that the above formulation is schematic and does not indicate the detail structure of the matrices due to the displacement boundary conditions and corresponding reactions.

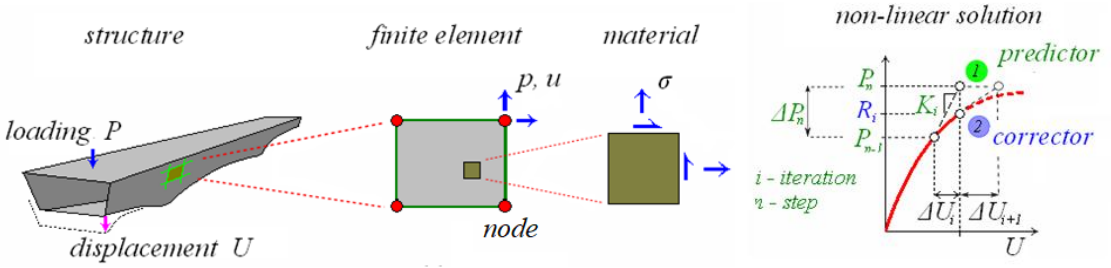

Fig. 15: Basic idea of the finite element method showing the discretization of the structure in finite elements, the evaluation of stresses at individual integration points, and the incremental solution predictor-corrector solution.

The non-linear response is solved in increments. In a load step, a displacement increment $\Delta U_{n,i}$ due to the load increment ΔP_n is estimated by the *predictor*, marked as point 1. It estimates the response based on the element stiffness matrix k, which is defined in the matrix format as follows:

$$\varepsilon = Bu, \;\; \sigma = D\varepsilon, k = \int_v \; B^T D \; B \; dv \tag{3}$$

where ε – element strains, σ – element stresses, B – strain-displacement matrix for given finite element formulation, u – element nodal displacements, k – element stiffness matrix. The Integration is performed over the volume of the finite element. The matrix B can also include high order terms and reflect the geometrical non-linearity. Matrix D is based on the linear elastic theory (with two parameters, elastic modulus and Poison's ratio). It is based on a tangent elastic modulus, but alternative methods are available based on other values. Eq.(3) follows form the theorem of minimum of total potential energy and more detailed derivation can be found, for example, in Zienkiewicz (1967).

Due to the linear approximation the solution obtained by the predictor differs from a nonlinear response. Therefore, a correct resistance is found by the *corrector* as follows:

$$\sigma = F(\sigma, \varepsilon), \; r = \int_v \; B^T \sigma \; dv \tag{4}$$

In this $F(\sigma, \varepsilon)$ – constitutive law, and r – vector of resisting nodal forces consistent with the constitutive law. The constitutive law is a function of stress and strain and typically include additional parameters. In this presentation two laws, based on the theories of plasticity and fracture are described.

In case of a unique solution the difference $P_n - R_{n,i}$ wannish and the iterative solution converges to a nonlinear response. The process can be refined by adopting methods to improve the iteration stability, such as the methods of line-search and arc-length.

4.2 Concrete Material Model with Time Dependent Properties

The essential part of the nonlinear finite element analysis are material models that can realistically describe the behavior of brittle cementitious material such as concrete. In the field of material science, this is mostly represented by a stress-strain constitutive relationship. The material model should respect the physics principles and in the case of brittle materials should properly consider the energy dissipated during the damage processes and volumetric dilation during concrete crushing. In order to simulate the behavior of "Green Concrete" with SCM replacement, which exhibits slower development of concrete strength, the concrete model should support the time dependent evolution of the key material parameters.

ATENA software package implements the fracture-plastic model proposed by Červenka J. et al. [10],[11],[17]. It divides the nonlinear material response into tension and compression.

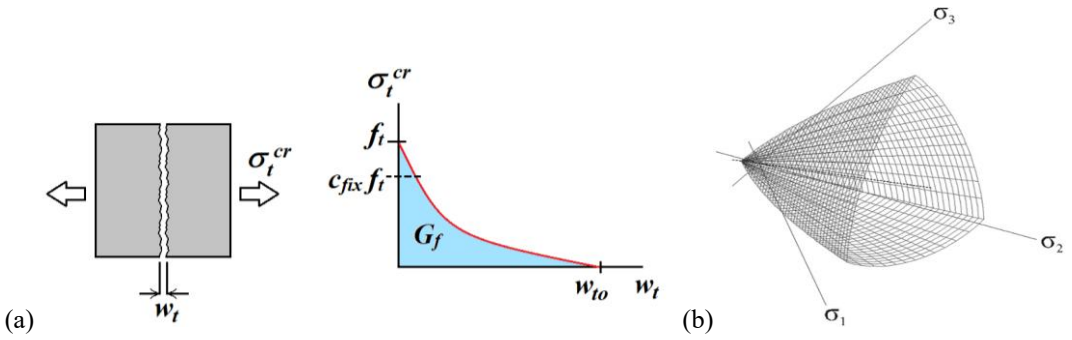

Fig. 16. Crack opening law that controls the softening response in tension (a) and 3D plasticity criterion for concrete crushing

The tensile post-peak response is characterized by an orthotropic smeared crack model with a softening curve controlled by the fracture energy that is dissipated during the crack propagation as shown in Fig. 16. Rather than explicitly tracking each individual crack, the smeared crack approach adds the response of multiple cracks within a single element and adequately modifies the strength and energy dissipation of the element. The cracking model is orthotropic and allows the formation of up to three cracks in the three principal material directions.

It has been observed that the smeared crack models suffer certain mesh dependency. For instance, if large elements in order of hundreds of millimeters or even meters are used in the model, the assumption that a single crack develops in a principal tension direction is no longer valid. Several cracks parallel crack my localize in the case of a reinforced concrete sample. Therefore, the total fracture energy available for dissipation is underestimated in the simulation thus reducing the peak load and incorrectly increasing the brittleness of the response. This can be adjusted by an additional material parameter specifying the crack spacing Fig. 16. Analogically, if a very small mesh is used, the number of cracks may be overestimated. The minimum crack spacing would be limited by the internal material length scale depending on the aggregate size [13]. By imposing a limit on minimum crack spacing, it can be ensured that the crack will localize in a physically plausible distance range.

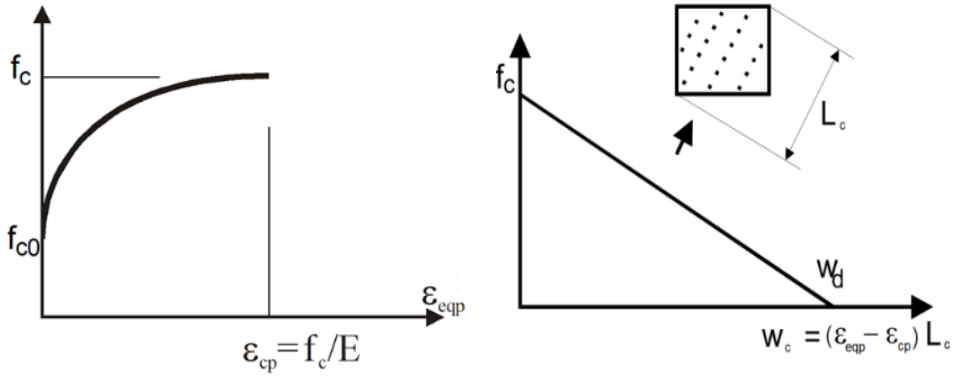

Fig. 17: Hardening/softening diagrams for the plasticity model for concrete in compression.

The compression branch is described by the plasticity approach with the Menetrey & Willam failure criterion [38] shown in Fig. 17. The figure shows the hardening elliptical curve after exceeding the stress level corresponding to the onset of crushing f_{c0} and linear softening after reaching the compressive strength. The material model incorporates a yield surface (Fig. 16) and non-associated flow rule to capture the plastic strain evolution during the concrete crushing.

When nonlinear material laws are introduced into the FEM, the set of equations to be solved becomes nonlinear. Therefore, a suitable solver technique is necessary to find the equilibrium between the nodal displacement and material response. Most commonly, these methods are derived from the well-known Newton-Raphson method. The iterative solution runs until the residual error decreases below the prescribed convergence criteria. Only the results, where the convergence of the solution was reached, should be used for structural analysis. The loss of convergence is sometimes an indicator that the ultimate load-bearing capacity was exceeded; however, the results should be always carefully inspected to determine the actual cause of the divergence.

Once the convergence at a given load step is obtained, the next load step is calculated based on the previously calculated state. Unlike in the linear (i.e., elastic) solution, the superposition principle is not valid, meaning that the structural response under multiple loadings cannot be found by simple addition. Therefore, the loading history plays an important role in the simulation and should resemble the actual loading scenario.

Most engineering applications are formulated as load-prescribed tasks since the design standards generally specify the external loads. For this purpose, the arc-length method [17] is more suitable as it scales the load vector based on the displacement increment. Thus, the applied load is automatically scaled down when the maximum load-carrying capacity is reached. The arc-length method allows tracing the structural response when the ultimate load-carrying capacity is reached into the post-peak behavior.

In the proposed methodology, the mechanical behavior of concrete is described by a constitutive law in which **material parameters evolve in time** to reflect the development of material properties during curing and ageing. In a general form, the constitutive relationship can be expressed as

$$\boldsymbol{\sigma}(t) = \mathcal{F}(\boldsymbol{\varepsilon}(t), \dot{\boldsymbol{\varepsilon}}(t), \boldsymbol{\alpha}(t), \mathbf{p}(t)) \tag{5}$$

where
$\boldsymbol{\sigma}(t)$is the stress tensor,
$\boldsymbol{\varepsilon}(t)$is the strain tensor,
$\dot{\boldsymbol{\varepsilon}}(t)$is the strain rate,
$\boldsymbol{\alpha}(t)$denotes a set of internal state variables (e.g. damage, plastic strains), and
$\mathbf{p}(t)$represents a vector of **time-dependent material parameters**.

The time dependence of material parameters is introduced through explicit functions of time or material maturity, such that

$$\mathbf{p}(t) = \mathbf{p}_0 \, g(t)$$

or, more generally,

$$\mathbf{p}(t) = \mathbf{p}(t, \Theta(t))$$

where $\mathbf{p}_0$denotes reference material parameters and $\Theta(t)$represents a maturity or ageing measure describing the evolution of material properties. Typical time-dependent parameters include elastic modulus, tensile and compressive strength, fracture energy, and hardening or softening parameters.

For practical applications, the evolution of material properties is commonly described by **material maturity curves** or directly by providing **empirical evolution functions** for **material parameters** calibrated from experimental data. These functions allow the constitutive response at any time $t$to be evaluated consistently with the current state of material development.

Within nonlinear analysis, the constitutive model is evaluated incrementally in time, with material parameters updated at each analysis step according to the prescribed evolution laws. This formulation enables the simulation of **construction stages, delayed strength development, and interaction between material ageing and structural loading**, which are essential aspects of the design and optimization of structures made of green concrete.

4.3 Safety Formats for Design by Numerical Simulation

For the application of nonlinear FE analysis in engineering practice, an appropriate safety framework needs to be available. The standard assessment formula specifies that the design structural resistance R_d must be greater than the effect of design loads E_d. Therefore:

$$E_\mathrm{d} < R_\mathrm{d} = \frac{R_\mathrm{d}^\mathrm{FE}}{\gamma_\mathrm{Rd}} \tag{6}$$

The fib Model Code [25] defines three kinds of nonlinear methods for obtaining the design structural resistance. These are the full probabilistic, global resistance, and partial factor methods (PFM).

The method closest to the traditional approach in cross-sectional design is the PFM. It specifies that the material parameters used in the nonlinear analysis are derived from the design values of the concrete compressive strength for concrete and reinforcement design yield strength or rapture strain. During the nonlinear simulation, the design load combination is gradually increased until the maximum load-bearing capacity R_d^{FE} is found. The maximum load value gives the global resistance R_d^{FE}, which should be further reduced by the model uncertainty partial safety factor γ_{Rd} to obtain the structural design resistance.

Another semi probabilistic global resistance approach is the estimate of the coefficient of variation (ECoV) originally proposed by Červenka V. [15][16]. It assumes that the design structural resistance follows the lognormal distribution, which can be characterized by the characteristic R_k and mean structural R_m resistances. From these, the coefficient of variation V_R can be estimated as:

$$V_\mathrm{R} = \frac{1}{1.65}\, ln\left(\frac{R_\mathrm{m}}{R_\mathrm{k}}\right) \tag{7}$$

and the global resistance factor γ_R is calculated using the assumption of lognormal distribution:

$$\gamma_\mathrm{R} = exp(\alpha_\mathrm{R}\, \beta\, V_\mathrm{R}) \tag{8}$$

where α_R is the sensitivity factor for resistance in MC 2010 [25] and EC2 [24] with a recommended value of 0.8 for a 50-year reference period. β is the target value for the reliability index typically 3.8 in MC 2010 and EC2 for a 50-year reference period. The design structural resistance according to the ECoV method is calculated:

$$R_\mathrm{d,ECOV} = \frac{R_\mathrm{m}}{\gamma_\mathrm{R}\, \gamma_\mathrm{Rd}} \tag{9}$$

The fib Model Code [25] also lists the full probabilistic method; however, this method will be quite demanding for typical engineering applications as it often requires hundreds of nonlinear analyses.

4.3.1 Model Uncertainties and Safety Factors

Model uncertainty is generally described as the ratio of the resistance found experimentally R_{exp} and the resistance obtained in the simulation R_{sim}:

$$\theta = \frac{R_\mathrm{exp}}{R_\mathrm{sim}} \tag{10}$$

It can be considered as a random variable that can be obtained by statistical evaluation of simulation results of various experiments. Assuming the lognormal distribution of the evaluated dataset, the safety factor for model uncertainty γ_{Rd} can be calculated as:

$$\gamma_{\mathrm{Rd}} = \frac{\exp(\alpha_{\mathrm{R}} \cdot \beta \cdot V_\theta)}{\mu_\theta} \tag{11}$$

where μ_θ is the mean value of the model uncertainty and V_θ is the coefficient of variation from the model uncertainty calculation. For the sensitivity factor for the reliability of resistance α_R and the reliability index β, values of 0.8 and 3.8 can be again taken from [23][25].

The model partial safety factor is specific to a given software package or material model. Furthermore, it may be dependent on the failure mode, i.e. bending, shear, or compression. For the ATENA software package [17] with the fracture-plastic material model [10][11], the model uncertainty is evaluated by a statistical analysis in the publication [16] for 33 typical cases of reinforced concrete structural elements with failure modes ranging from bending, shear and punching failure mechanisms.

Tab. 1: Recommended model uncertainty partial factor for ATENA software [16].

Failure mode	μ_θ	V_θ	γ_{Rd}
Bending mode	1.072	0.052	1.01
Shear failure	0.984	0.067	1.13
Punching failure	0.971	0.076	1.16
All modes	0.979	0.081	1.16

Similar model uncertainty studies have been performed for other models and finite element software codes by other researchers such as for instance Engen [22], Castaldo [4][5] and Gino [27]. The obtained uncertainty factors were mostly in the range 1.02 – 1.19 except for the study [5], which included also cyclic load cases, and the model uncertainty factor 1.35 was obtained.

4.4 Modelling and Design of Optimized Construction Sequence for Green Concrete Materials

The general approach for the optimization of construction sequence and the selection of suitable concrete type can be summarized into the following steps:

Step 1: Estimation of time history of stress and internal forces development in the critical sections and concrete elements.

For each critical section/element, determine the time-dependent **design action effect** (stress resultant or stress measure) generated by the staged construction sequence $\mathbf{s}$:

$$E_d(t;\mathbf{s}) = \mathcal{E}(\mathbf{F}_d(t;\mathbf{s}), \mathrm{BC}(t;\mathbf{s})), \sigma_d(t;\mathbf{s}) = \mathcal{S}(E_d(t;\mathbf{s})) \tag{12}$$

where $\mathbf{F}_d(t;\mathbf{s})$represents the time-dependent design actions (self-weight, handling/erection loads, temporary supports, prestressing, imposed loads, etc.) in the relevant combinations and $\mathrm{BC}(t;\mathbf{s})$denotes stage-dependent boundary conditions.

Step 2: Map stress history development into the green concrete database of material maturity curves.

Using the material database for mixture m, introduce the maturity (or equivalent age) function $\Theta(t)$ and evaluate time-dependent material properties:

$$f_{c,m}(t) = f_{c,m}(\Theta(t)), f_{t,m}(t) = f_{t,m}\,(\Theta(t)), E_m(t) = E_m(\Theta(t)) \quad (13)$$

These functions provide the **age-dependent resistance basis** for all critical construction stages.

Step 3: Select suitable material and optimize the construction sequence.

Formulate the construction-stage verification in the standard "actions vs. resistance" format required for all critical times/stages $t \in \mathcal{T}_{\text{crit}}$:

$$E_d(t;\mathbf{s}) \le R_d(t;m) \Leftrightarrow \eta(t;\mathbf{s},m) = \frac{E_d(t;\mathbf{s})}{R_d(t;m)} \le 1 \forall t \in \mathcal{T}_{\text{crit}} \quad (14)$$

with age-dependent design resistance defined using partial factors (Eurocode/fib concept):

$$R_d(t;m) = \frac{R_k(t;m)}{\gamma_M}, R_k(t;m) \text{ derived from } f_{c,m}(t), f_{t,m}(t), E_m(t) \quad (15)$$

The "optimized" pair $(m, \mathbf{s})$ is then selected as a feasible solution satisfying $\eta(t) \le 1$ while meeting the chosen project objective (e.g. minimum CO_2, cost, or construction duration).

Step 4: Verify the selected material and construction sequence by numerical simulation in ATENA-Green Concrete Module.

Perform staged nonlinear numerical simulation with step-wise updates of actions, boundary conditions, and material parameters:

$$s \Rightarrow \mathbf{F}_d(t), \mathbf{BC}(t); \quad m \Rightarrow p(t) = \{f_{c,m}(t), f_{t,m}(t), E_m(t), \dots\}$$

and verify that the governing criteria remain satisfied in all relevant stages (e.g. limit-state checks expressed by $\eta(t) \le 1$, cracking/damage indicators, and serviceability measures), thereby confirming the adequacy of the selected mixture and construction schedule.

5 Example of Application

This section presents a **representative example of application** of the proposed Green Concrete Design and Optimization Methodology to a selected New-MRCS structural system. The purpose of the example is to illustrate the **practical use of the methodology** and to demonstrate how the individual steps described in the previous sections can be combined into a coherent design and decision-making process.

The example follows the **four-step procedure based on numerical simulation**, including estimation of stress development during the construction sequence, consideration of time-dependent material properties, selection and optimisation of concrete material and construction stages, and final numerical verification. The example is not intended to cover all possible design scenarios, but rather to highlight **typical modelling assumptions, critical decisions, and interpretation of results** relevant for engineering practice.

By documenting the workflow and key outcomes, the example serves as a **practical guide for applying the methodology** and illustrates its applicability to prefabricated systems incorporating green concrete with increased SCM content.

5.1 Example of Column-Beam Connection Modelling and Design

This example illustrates the application of the ATENA Module for Green Concrete Modelling and Design to the **nonlinear analysis and design verification of a reinforced concrete column–beam connection**. The example represents a typical structural detail encountered in building structures and demonstrates the practical use of the software developed for **engineering assessment and design-oriented evaluation**.

The analyzed detail (see Fig. 18) represents a typical composite steel-concrete connection with multi-spiral reinforcement, as investigated in this project and developed by the Taiwanese partners. Such a connection has also been extensively modelled and tested during this project. The strength of the detail as well as its behavior during cycling loading has been extensively studied and validated by other workpackages and developed software tools. Namely the project software outcome V1 [20] and paper [42] describes this aspect of the project in more detail. The model of the analyzed column-beam connection design can be parametrically generated using the other developed ATENA module for MRCS parametric modelling and design [20].

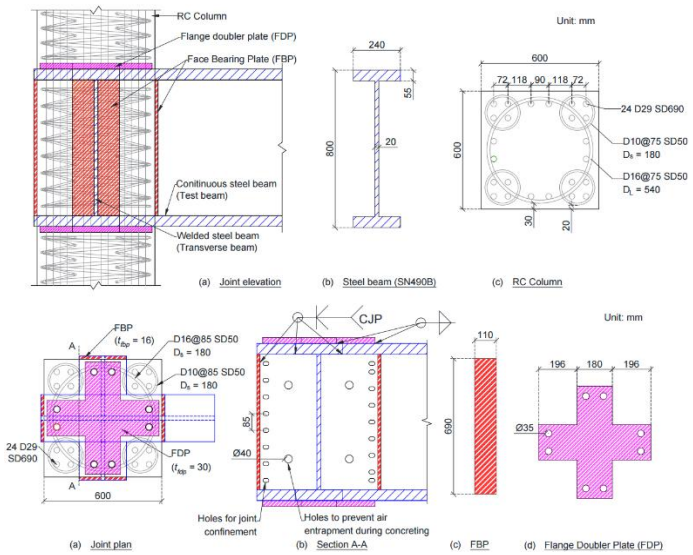

Fig. 18: The detail of the steel-concrete MRCS connection used as an example for Green Concrete modelling and simulation.

The analyzed column–beam connection is modelled using a three-dimensional nonlinear finite element representation, including concrete, reinforcement, and bond interaction. The behavior of concrete is described using the fracture–plastic constitutive model implemented in ATENA and extended within the CeSTaR-3 project to account for **green concrete with supplementary cementitious materials (SCMs)**. Material parameters may be derived from experimentally validated data, including values available in the experimental database **TM04000013-V6**, ensuring consistency between experimental observations and numerical modelling.

The numerical model captures the key mechanisms governing the response of the connection, including:

- cracking and crushing of concrete in the joint region,
- nonlinear behavior of longitudinal and transverse reinforcement,
- stress redistribution between the beam and column under increasing load,
- interaction between bending, shear, and axial forces.

This example confirms that the ATENA Module for Green Concrete Modelling and Design can be effectively used for **modelling, analysis, and design-oriented assessment of structural connections**, which are critical components of reinforced concrete structures. The demonstrated workflow highlights the applicability of the software for practical engineering tasks involving green concrete materials, bridging experimental research results and everyday design practice.

In this example, the detail of the connection is modelled as being part of a bigger structure, and being located at the 22th floor of the analyzed building, i.e. 4th level from the top (see Fig. 19).

This example problem will model the connection detail. The numerical model is shown in Fig. 20. The loads on this connection detail will be gradually applied to simulate the loads coming from the top floors, and they will simulate the gradual building construction. The application of loads is slightly simplified such that the focus is placed on the development of the material strength in relation to the gradual increase of loads rather than on the complexity of the real life construction process and the required design verifications. In this example scenario, the following load history is assumed as listed in Tab. 2.

Fig. 19: View of the whole building and the typical steel-concrete MRCS connection detail.

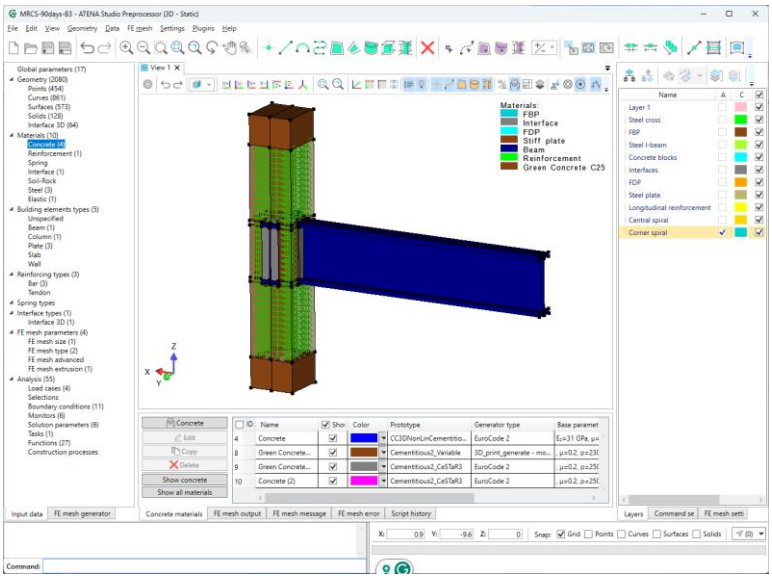

Fig. 20: View of the column-beam connection model in the software window.

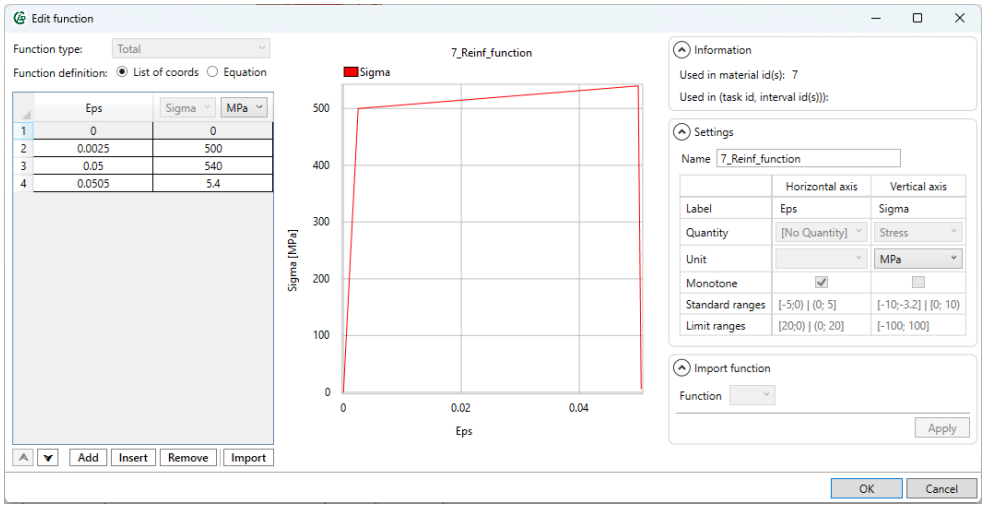

Fig. 21: Reinforcement stress-strain diagram used in the MRCS example.

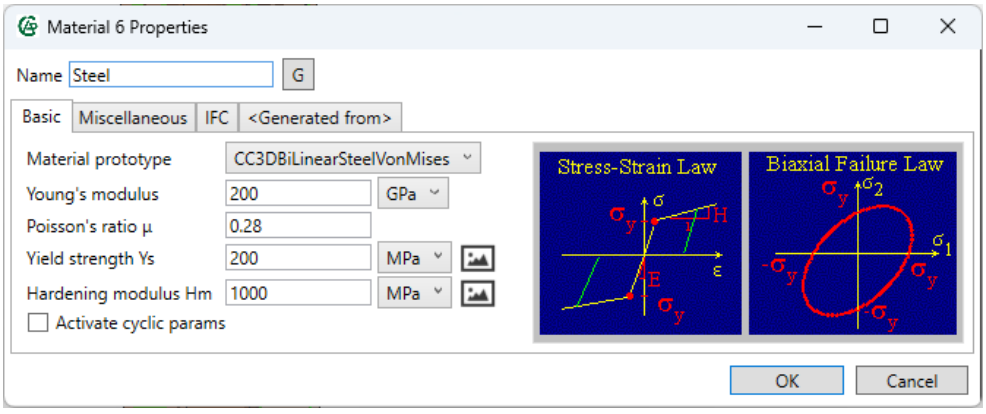

Fig. 22: Steel member material properties used in the MRCS connection example.

Tab. 2: Loading history applied in column-beam example problem

Int.	Name	# Steps	Duration [days]	Description
1	Detail dead load	1	5	Application of dead load from level I construction.
2	Beam load	5	5	Application of loads on steel beams from level I construction
3	Level II construction	1	10	Construction of Level II
4	Formwork removal	5	1	Increase of top column loads due to level II construction 2.88MN.
5	Level III construction	1	10	Construction of Level III
6	Formwork removal	5	1	Increase of top column loads due to level III construction 2.88MN.
7	Level IV construction	1	10	Construction of Level IV
8	Formwork removal	5	1	Increase of top column loads due to level IV construction 2.88MN.
9	Add. construction	5	90	Gradual increase of column forces by 0.72 MN due to additional construction

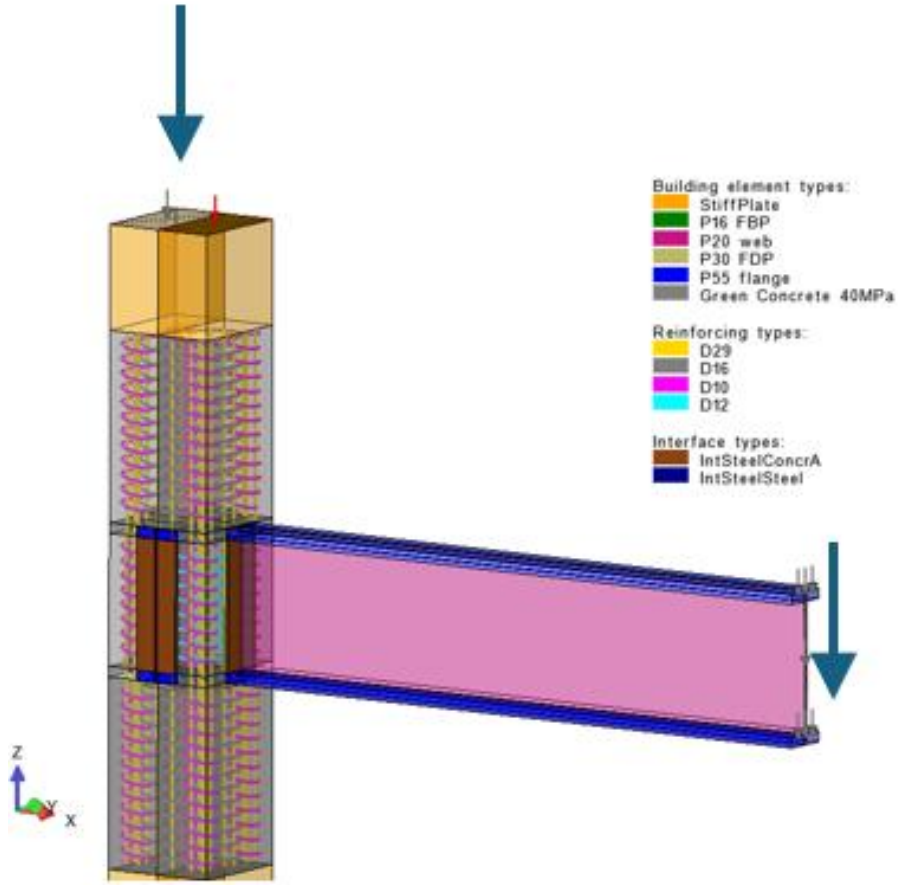

Fig. 23: Load application on the MRCS detail to simulate the loading from the rest of the structure.

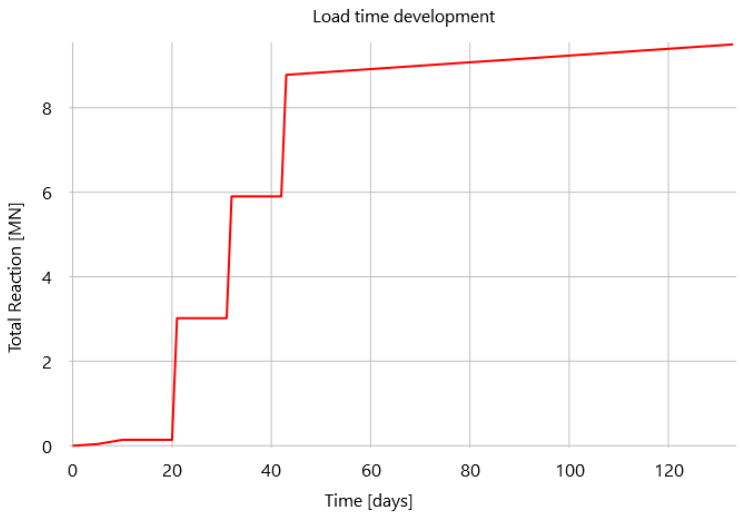

Fig. 24: The evolution of total reaction at the bottom of the column-beam MRCS detail simulating the gradual application of loads simulating the construction process.

The general approach for the optimization of construction sequence and the selection of suitable concrete type can be summarized into the following steps:

Step 1: Estimation of time history of stress development in the critical concrete elements.

Step 2: Map stress history development into the green concrete database of material maturity curves.

Step 3: Select suitable material and optimize the construction sequence.

Step 4: Verify the selected material and construction sequence by numerical simulation in ATENA-Green Concrete Module.

The proposed methodology [9] can be applied to the proposed example problem of a single column-beam MRCS connection detail as shown in Fig. 19 and Fig. 20. The application of the presented approach is described in the following subsections.

5.1.1 Step 1: Estimation of time history of stress development in the critical concrete elements.

The proposed loading history from Tab. 2 is applied to the MRCS connection detail that has been previously generated and validated using the project result V1 [20]. The numerical model is shown in Fig. 23. The average stresses in the connection are monitored and plotted in Fig. 25. The figure shows the vertical average stress development in time and is compared with the maturity curves of selected Green Concrete types from the database. The maturity curves of the green materials show the development of concrete design strength in time. The design concrete strength is determined from the material maturity curves by applying the appropriate material partial safety factors as described in the Green Concrete Modelling and Design Methodology developed in the project result V5 [9].

5.1.2 Step 2: Map stress history development into the green concrete database of material maturity curves.

From Fig. 25, it can be concluded that material labeled as PFA50 or GGBS50 are possible candidates to be used for the connection detail construction. The other possible candidate would be also the material labeled as LC15. However, the overall strength of this material might not be sufficient for subsequent live or extreme loads. The verification of live or extreme loads is not the subject of this study, which mainly focuses on the verification and optimization of the construction process and the selection of suitable material. The verification of all other required

design load combinations is an essential part of the design process and may be decisive for the selection of the most suitable concrete material. In these cases, however, only the final long term concrete material strength is important, and it is therefore out of scope of this project focus.

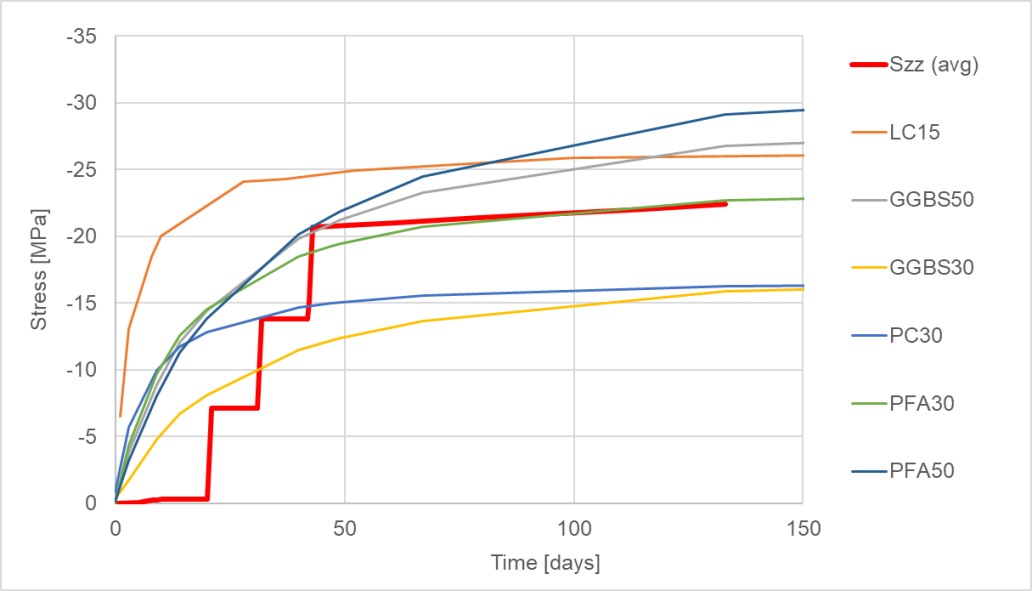

Fig. 25: Stress development in the concrete parts compared with the strength development of various Green Concrete types.

5.1.3 Step 3: Select suitable material and optimize the construction sequence.

Based on the Step 2, it was decided to choose the materials labeled as PFA30 or GGBS50 to be considered in the proposed design.

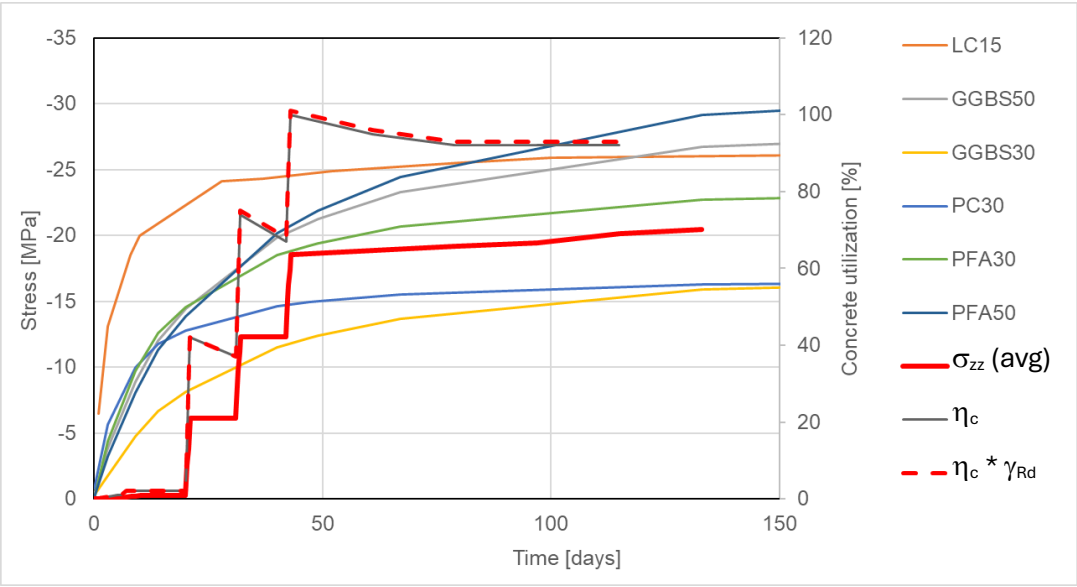

Fig. 26: Concrete stress and utilization evolution for the material PFA30

The figure shows that in terms of stress evolution the material PFA30 will closely satisfy the required stress evolution, however when the utilization factor is evaluated taking into account the required model uncertainty factor. According to the previous study [16] and the methodology [9] the smallest required model uncertainty factor γ_{Rd} = 1.01 can be used. The utilization factor in this case becomes slightly over 100%, so this material is not applicable unless the construction sequence is optimized.

This is documented on the following Fig. 27 where the average concrete stress and utilization levels are displayed for the case when the construction sequence is optimized (see Tab. 3).

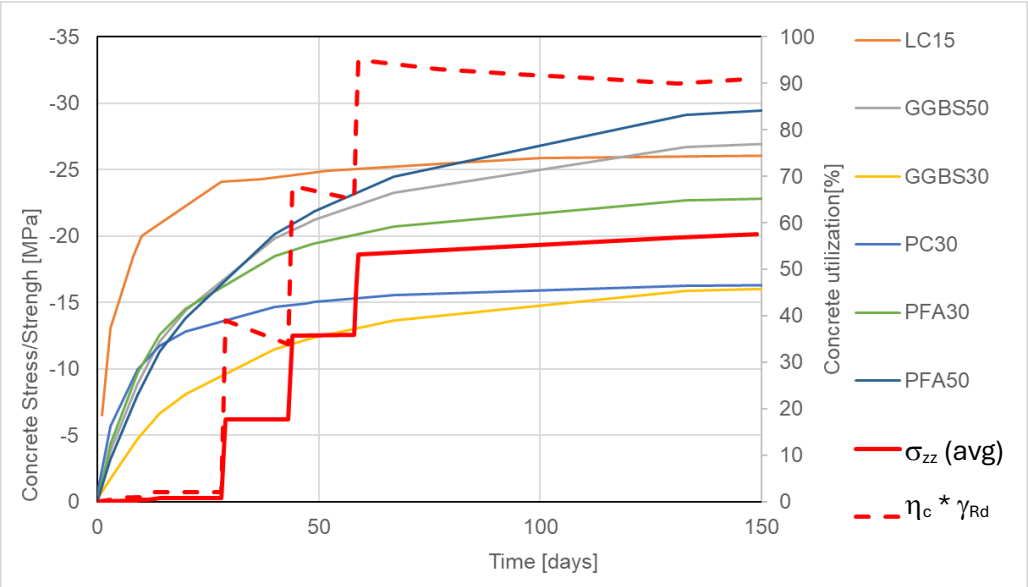

Fig. 27: Concrete stress and utilization evolution for the material PFA30 with optimized construction sequence.

Tab. 3: Optimized loading history applied in column-beam example for material PFA30

Int.	Name	# Steps	Duration [days]	Description
1	Detail dead load	1	5	Application of dead load from level I construction.
2	Beam load	5	5	Application of loads on steel beams from level I construction
3	Level II construction	1	10	Construction of Level II
4	Formwork removal	5	1	Increase of top column loads due to level II construction 2.88MN.
5	Level III construction	1	10	Construction of Level III
6	Formwork removal	5	1	Increase of top column loads due to level III construction 2.88MN.
7	Level IV construction	1	10	Construction of Level IV
8	Formwork removal	5	1	Increase of top column loads due to level IV construction 2.88MN.
9	Add. construction	5	90	Gradual increase of column forces by 0.72 MN due to additional construction

The other possibility would be to use the material labeled as GGBS50. The results for this case using the original loading history Tab. 2 is shown in Fig. 28.

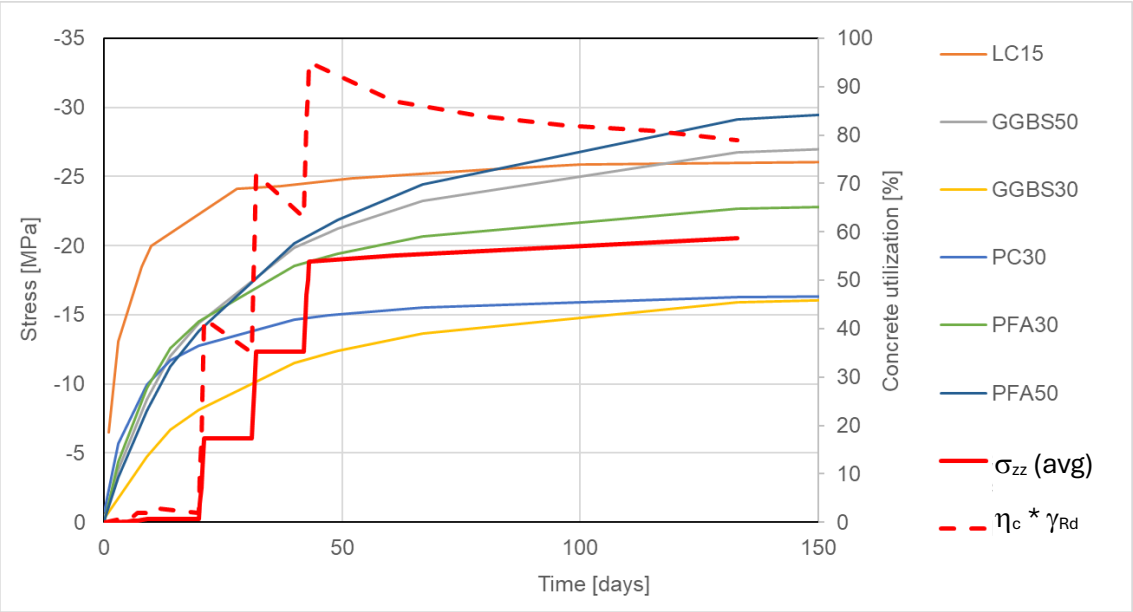

Fig. 28: Concrete stress and utilization evolution for the material GGBS50 with the original construction sequence.

5.1.4 Step 4: Verify the selected material and construction sequence by numerical simulation in ATENA-Green Concrete Module.

In this case, it can be decided to use the material GGBS50 since it shows reasonable concrete utilization levels. It is interesting to note that even though the average stress level in the connection is increasing in time as shown in Fig. 28 in times from 50 – 150 days, the overall utilization level is decreasing. This is due to the fact that the green concrete material is slowly maturing while stresses are still slightly increasing due to the continuing construction.

The final checks of the structural behavior at the early stages should involve checking the level of concrete stresses (see Fig. 31). It should be noted that higher stress than the current concrete strength can be observed due to stress localization namely in the sharp corner between concrete and steel elements. However, the concrete should not reach the crushing state, which in ATENA software can be documented by the softening flag in the Yield/Crush Info – Softening flag as shown in Fig. 30.

Another important quantity to check is the cracking in concrete during the construction. The crack widths should be limited to micro-cracks that are barely visible. Crack widths and cracking pattern for the selected material GGBS50 are shown in Fig. 31. It demonstrates that the crack widths are below 0.03 mm. The visibility crack limit is 0.05 mm and the typical crack limit in concrete design is 0.3 mm. It is clear that the concrete cracking is satisfying both these limits.

The other quantities that should be checked are stresses in the steel members of the MRCS connection as well as the stresses in the reinforcement. In this case, they are clearly below the yielding strength of the steel σ_y = 200 MPa and f_{sy} = 500 MPa for reinforcement.

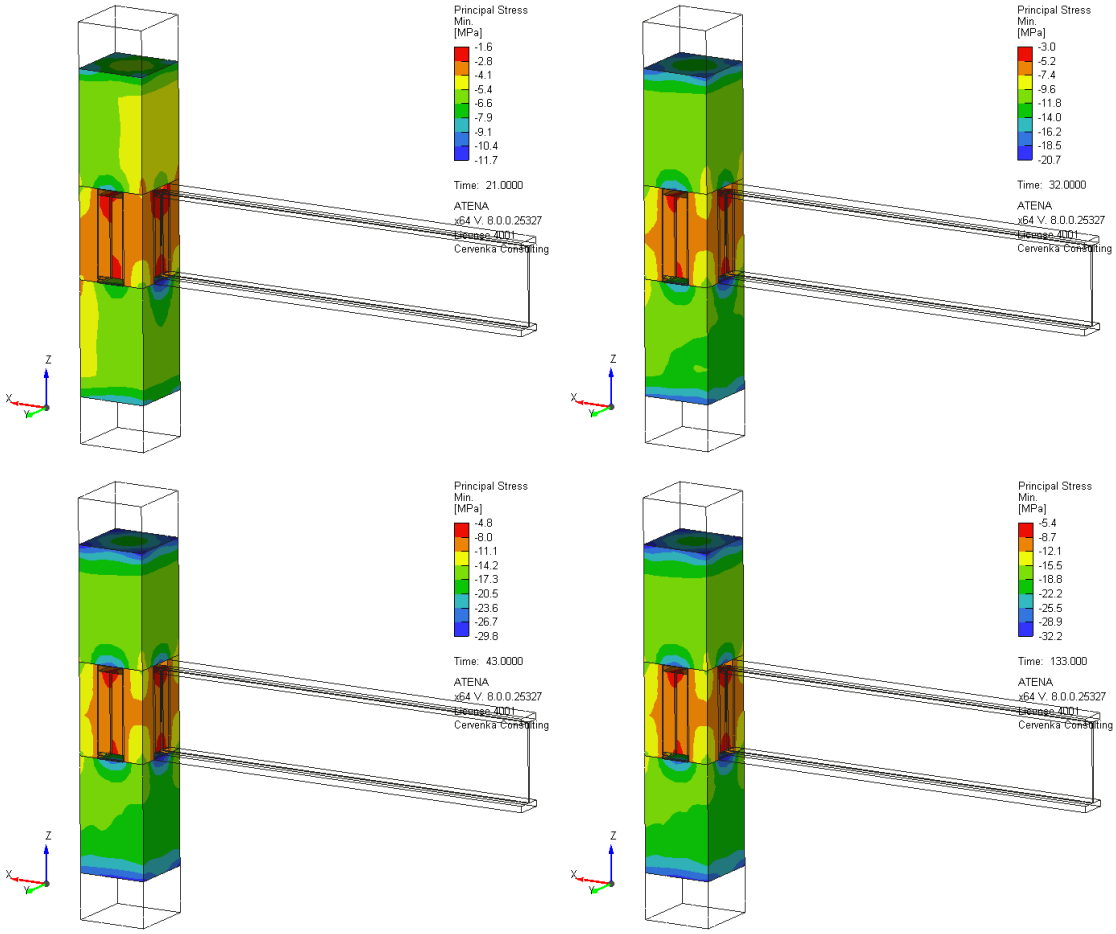

Fig. 29: Evolution of maximal concrete compressive stresses in the MRCS connection.

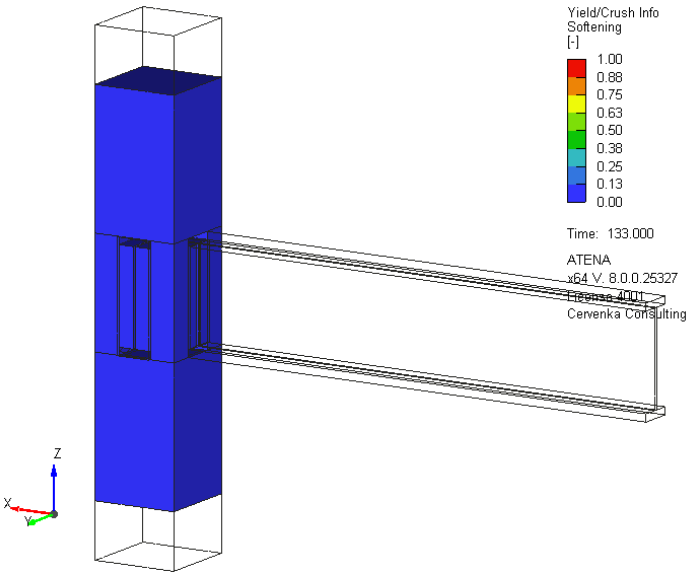

Fig. 30: Yield/Crush Info – Softening glag equal to 1 would indicate concrete crushing.

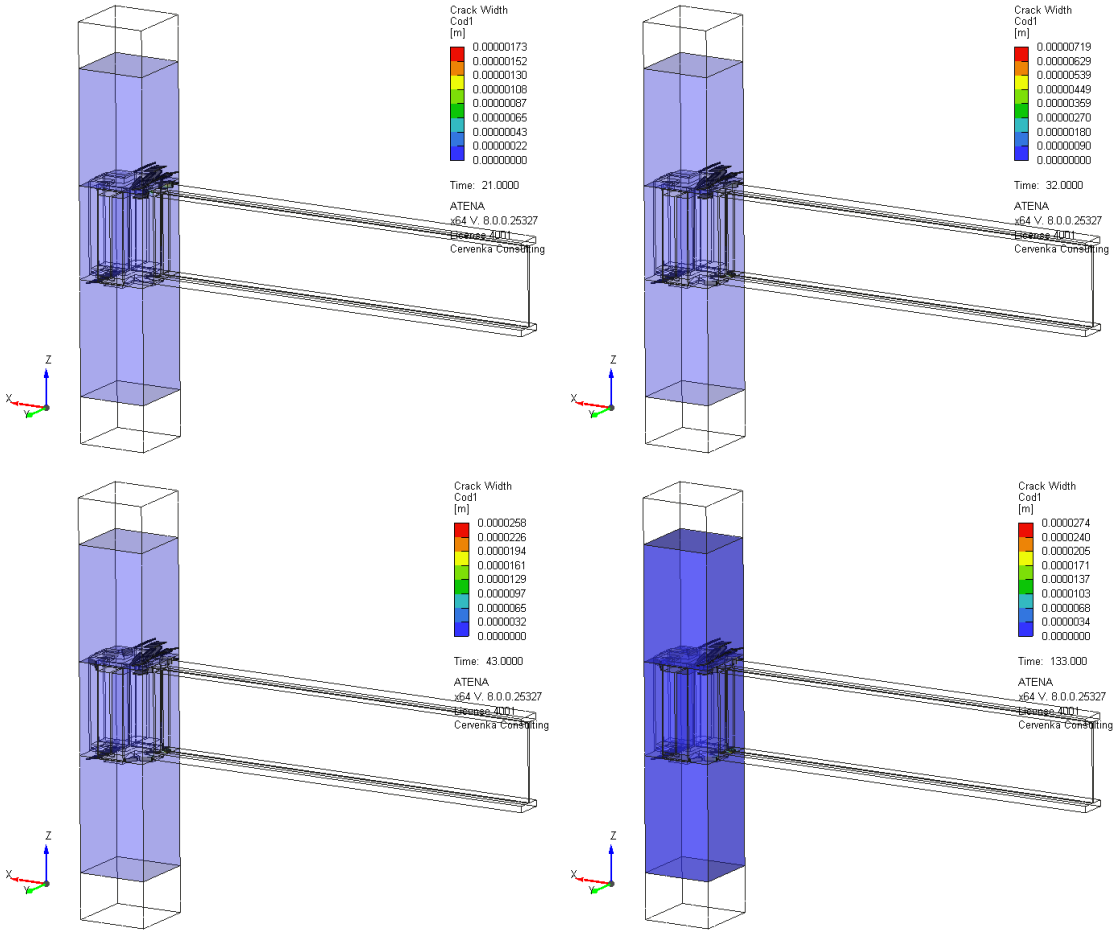

Fig. 31: Time evolution of concrete cracking in the MRCS connection during the construction process.

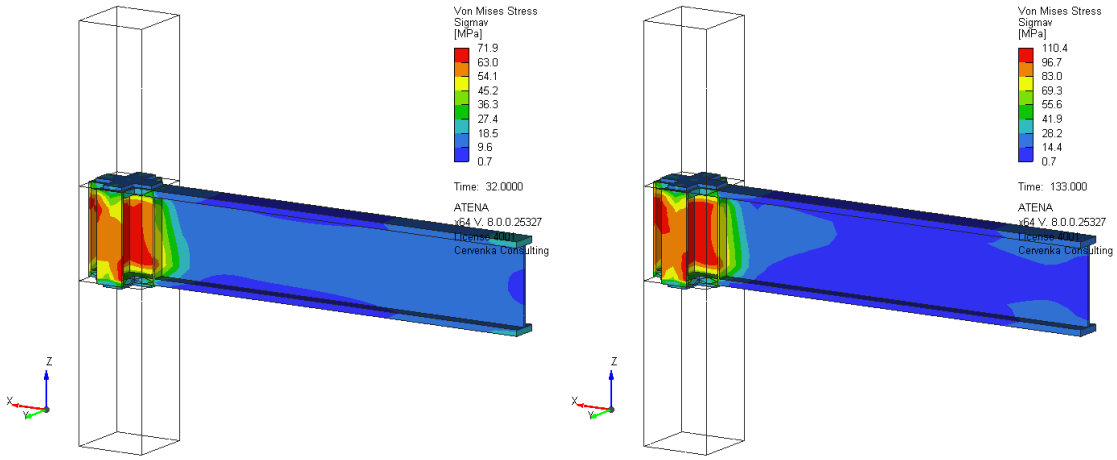

Fig. 32: Evolution of steel stresses in the MRCS connection for the material GGBS50.

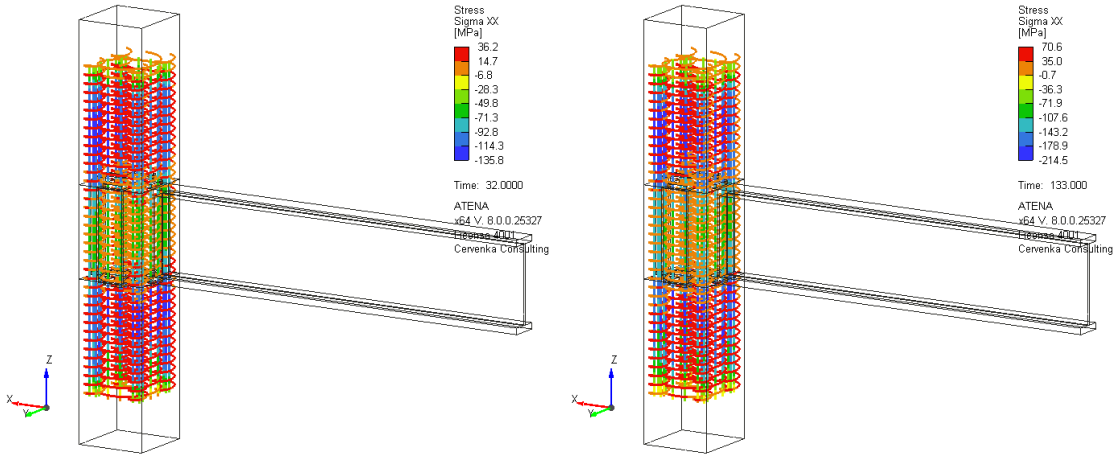

Fig. 33: Evolution of reinforcement stress in the MRCS connection for the material GGBS50.

5.2 Example of Composite Frame Modelling and Design

The next example uses the same MRCS connection detail, but this time it demonstrates and validates its application in a larger example, where the MRCS connections are part of a small composite steel concrete frame, which represents a selected part of the typical pilot building as shown in Fig. 19. The numerical model is shown in Fig. 34. It involves a MRCS connection detail as described in Section 5.1. The frame model consists of two levels with the floor height of 4.3 m and span between columns of 9.82 m in y direction and 10 m in x direction.

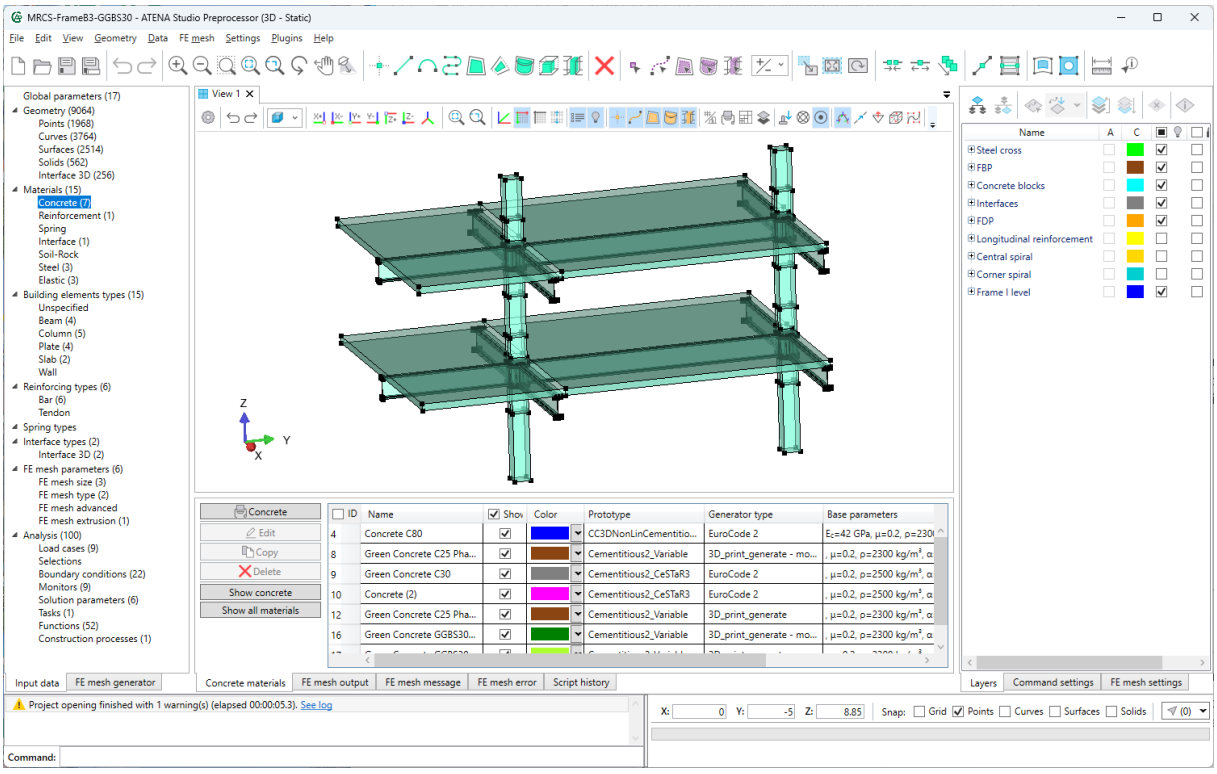

Fig. 34: Model of a small frame using MRCS connections in ATENA software with Green-Concrete construction process module.

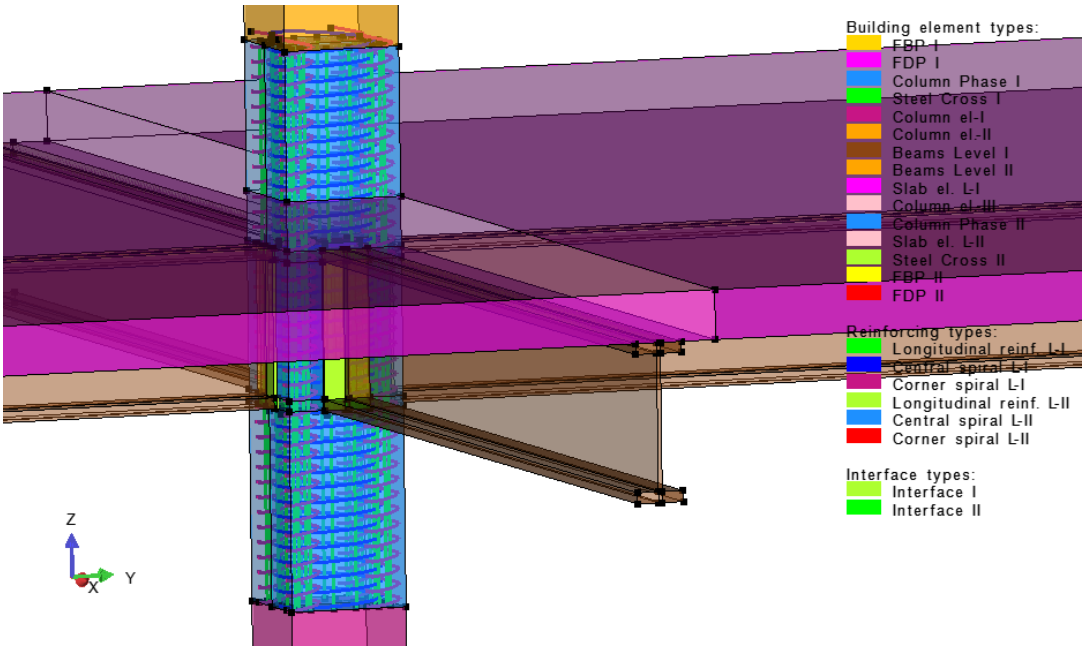

Fig. 35: Detailed reinforcement model at each MRCS connection.

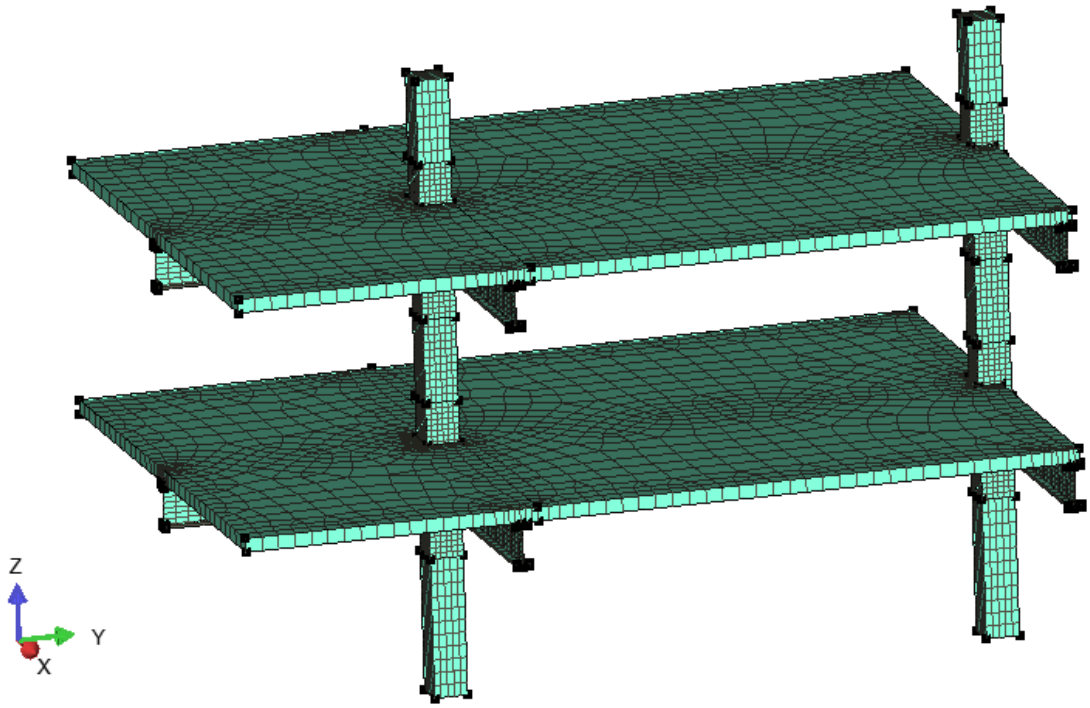

Fig. 36: Finite element model for the frame segment.

Tab. 4: Loading history applied in the frame segment example problem

Int.	Name	# Steps	Duration [days]	Description
1	Level I – Construction	1	7	Application of part of dead load for level I construction.
2	Level I – DL application, temporary supports removed	5	1	Application of remaining dead loads for level I construction
3	Level II – Construction	5	7	Applications of Level II construction loads to Level I.
4	Level II – DL application, temporary supports removed	5	1	Application of remaining dead loads for level II construction, load activation to Level – II elements.
5	Level III – Construction	5	7	Applications of Level III construction loads to Level I + II.
6	Level III – DL application, temporary supports removed	5	1	Application of remaining dead loads for level III construction, load activation to Level – III elements.
7	Additional construction	5	100	Remaining construction loads

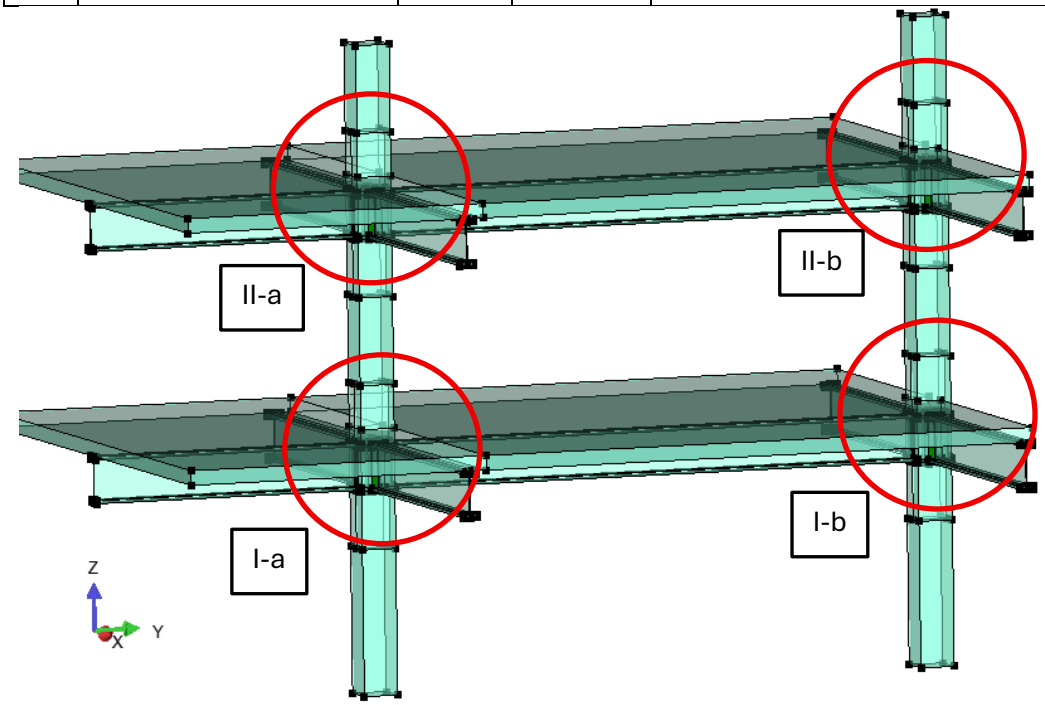

Fig. 37: Location and labeling of critical sections to be evaluated during the construction sequence and Green Concrete material optimization.

The general approach for the optimization of construction sequence and the selection of suitable concrete type according to the methodology [9] can be summarized into the following steps:

Step 1: Estimation of time history of stress development in the critical concrete elements.

Step 2: Map stress history development into the green concrete database of material maturity curves.

Step 3: Select suitable material and optimize the construction sequence.

Step 4: Verify the selected material and construction sequence by numerical simulation in ATENA-Green Concrete Module.

5.2.1 Step 1: Estimation of time history of stress development in the critical concrete elements.

The proposed loading history from Tab. 4 is applied to the frame segment with MRCS connections following the methodology [9] proposed in CeSTaR-3 project. The used numerical model is shown in Fig. 36.

In this case, two new features of the new ATENA – CeSTaR-3 Green Concrete module will be utilized:

- Modelling and simulation of material maturing and time development of material parameters.
- Modelling of construction process, i.e. gradual activation of various parts of the numerical model and their corresponding loads.

5.2.2 Step 2: Map stress history development into the green concrete database of material maturity curves.

The average stresses in the investigated connections are monitored and plotted in Fig. 38. The figure shows the vertical average stress development at each connection depending on the age of each element and is compared with the maturity curves of selected Green Concrete types from the database.

The maturity curves of the green materials show the development of concrete design strength in time. The design concrete strength is determined from the material maturity curves by applying the appropriate material partial safety factors as described in the Green Concrete Modelling and Design Methodology developed in the project result V5 [9].

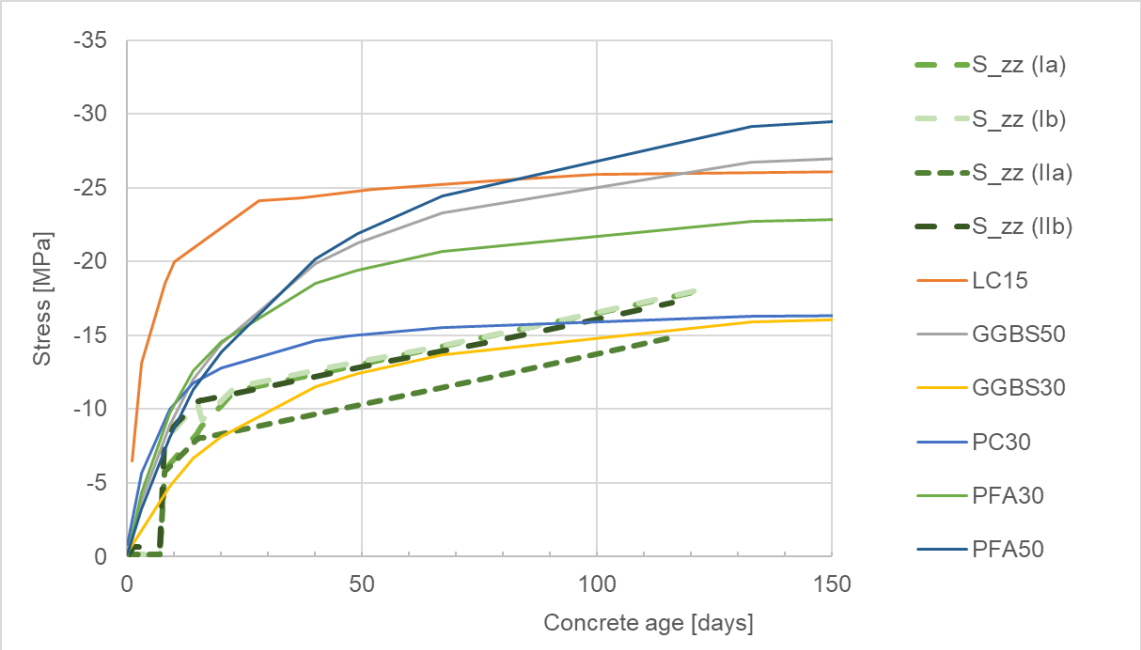

Fig. 38: Stress development in the concrete parts compared with the strength development of various Green Concrete types. The dashed lines show the average concrete stress development in the investigated MRCS connections (I-a to II-b, see Fig. 37). Horizontal axis is time in days from the beginning of each level construction.

5.2.3 Step 3: Select suitable material and optimize the construction sequence.

Based on the Step 2 and , it is possible to select suitable candidates for Green Concrete material. It is decided to choose the materials labeled as PFA30 or GGBS30 to be considered in the proposed design.

Fig. 39 shows the evolution of concrete stresses at each connection labeled Ia to IIb (see Fig. 37) based on the age of each element.

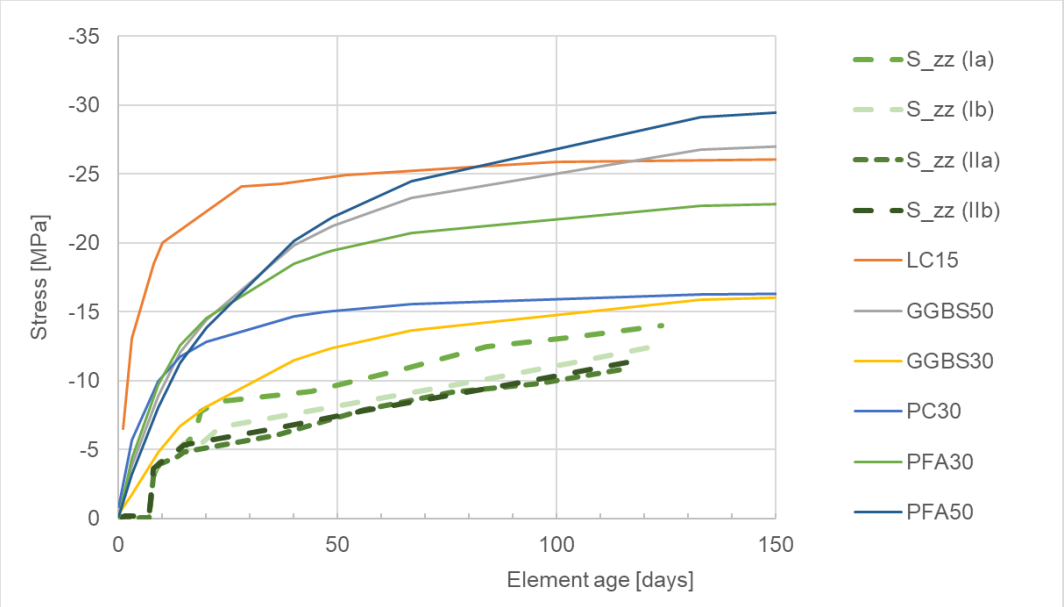

Fig. 39: Concrete stress evolution according to age at each connection detail for the material GGBS30.

The concrete utilization at each connection is shown in Fig. 40. It shows that the connection I-a has a utilization level higher than 100% at day 20 during the construction. This could addressed by modifying the construction sequence, i.e. increase the construction time of level II or by using another Green Concrete material.

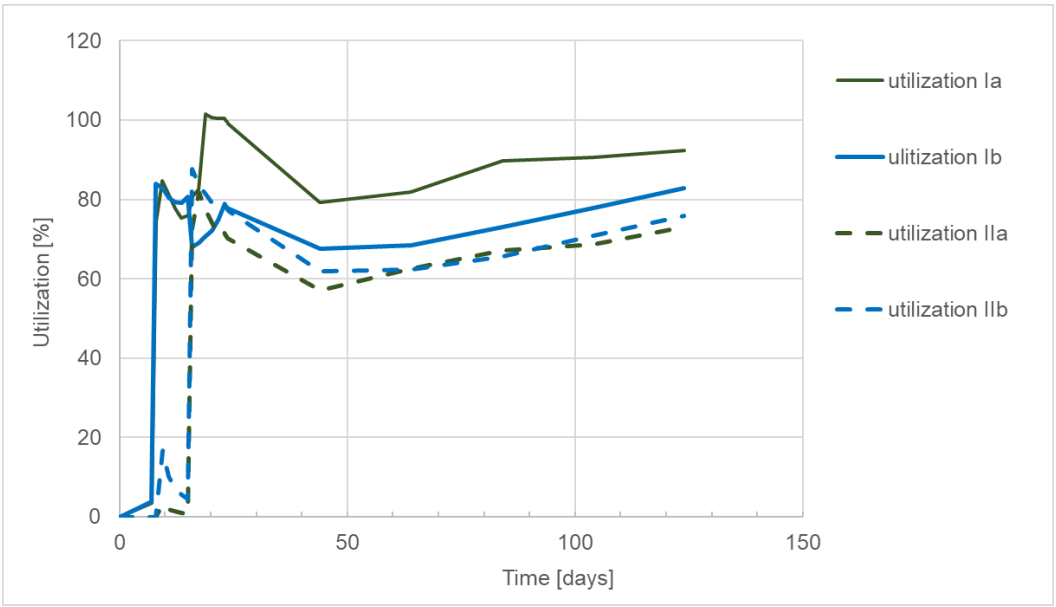

Fig. 40: Utilization of concrete at investigated connections during the construction process for the material GGBS30.

The results for different material PFA30 is shown in

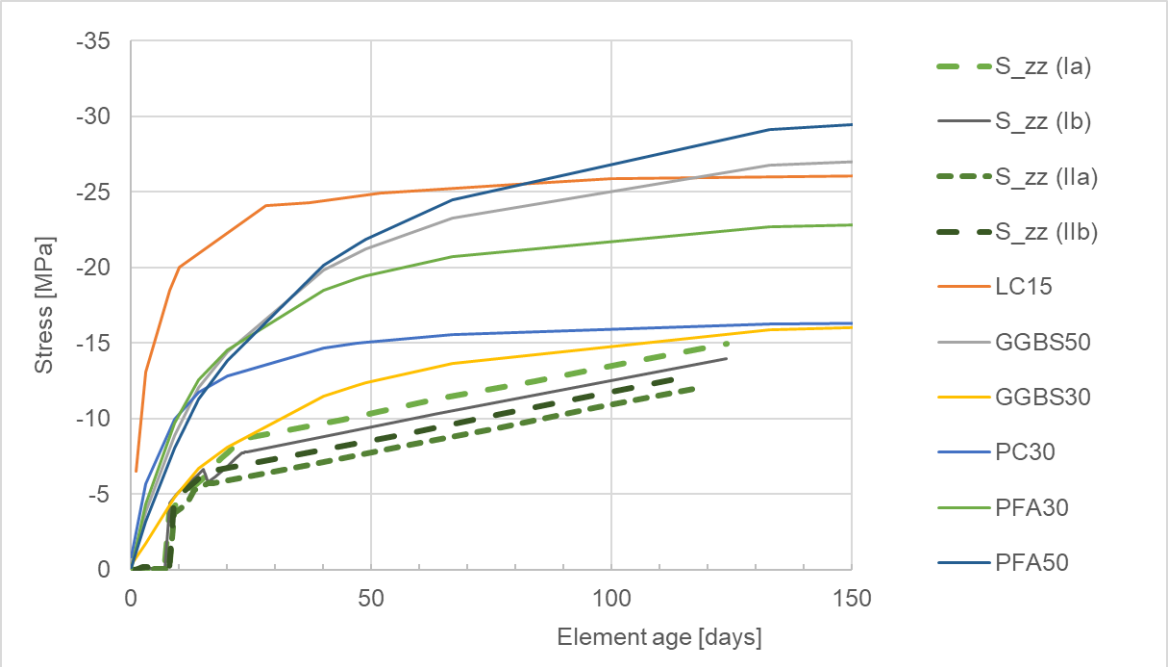

Fig. 41: Concrete stress evolution according to age at each connection detail for the material PFA30.

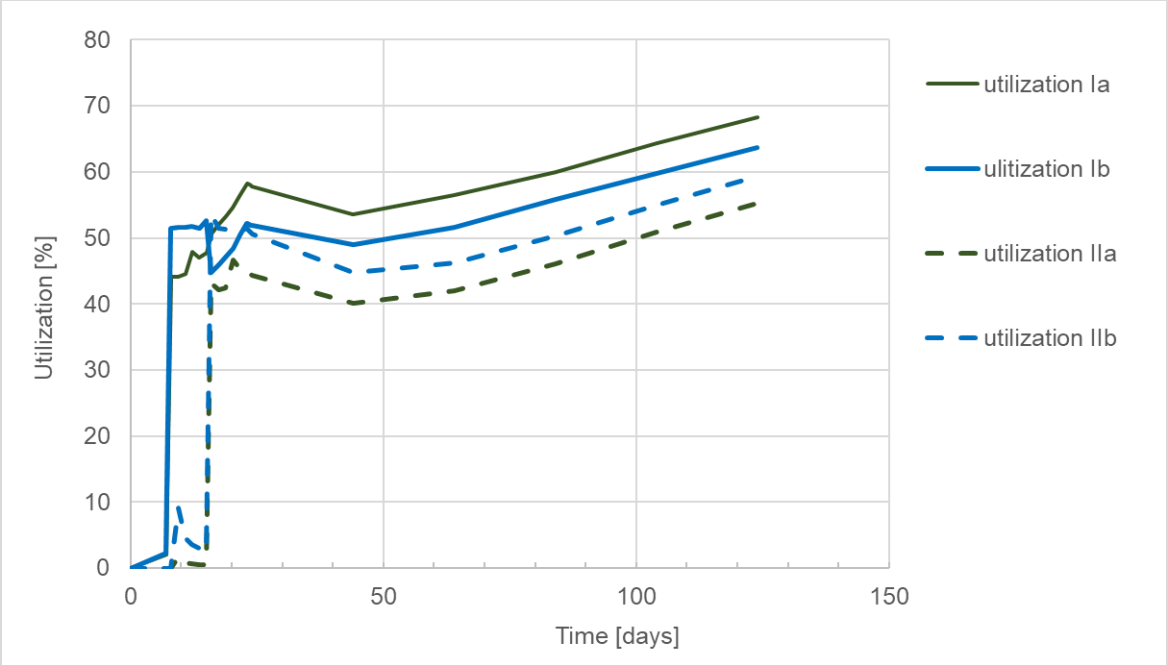

Fig. 42: Utilization of concrete at investigated connections during the construction process for the material PFA30.

5.2.4 Step 4: Verify the selected material and construction sequence by numerical simulation in ATENA-Green Concrete Module.

In this case, it can be decided to use the material PFA30 since it shows reasonable concrete utilization levels. It is interesting to note that even though the average stress level in the connection is increasing in time as shown in Fig. 41 in times from 20 – 150 days, the overall utilization level is not always increasing. It is possible to observe a partial decrease between day

20 to 50. This is since the green concrete material is slowly maturing while stresses are still slightly increasing due to the continuing construction.

Fig. 43 shows the evolution of deflections and the activation of various parts of the model in the construction sequence modelling.

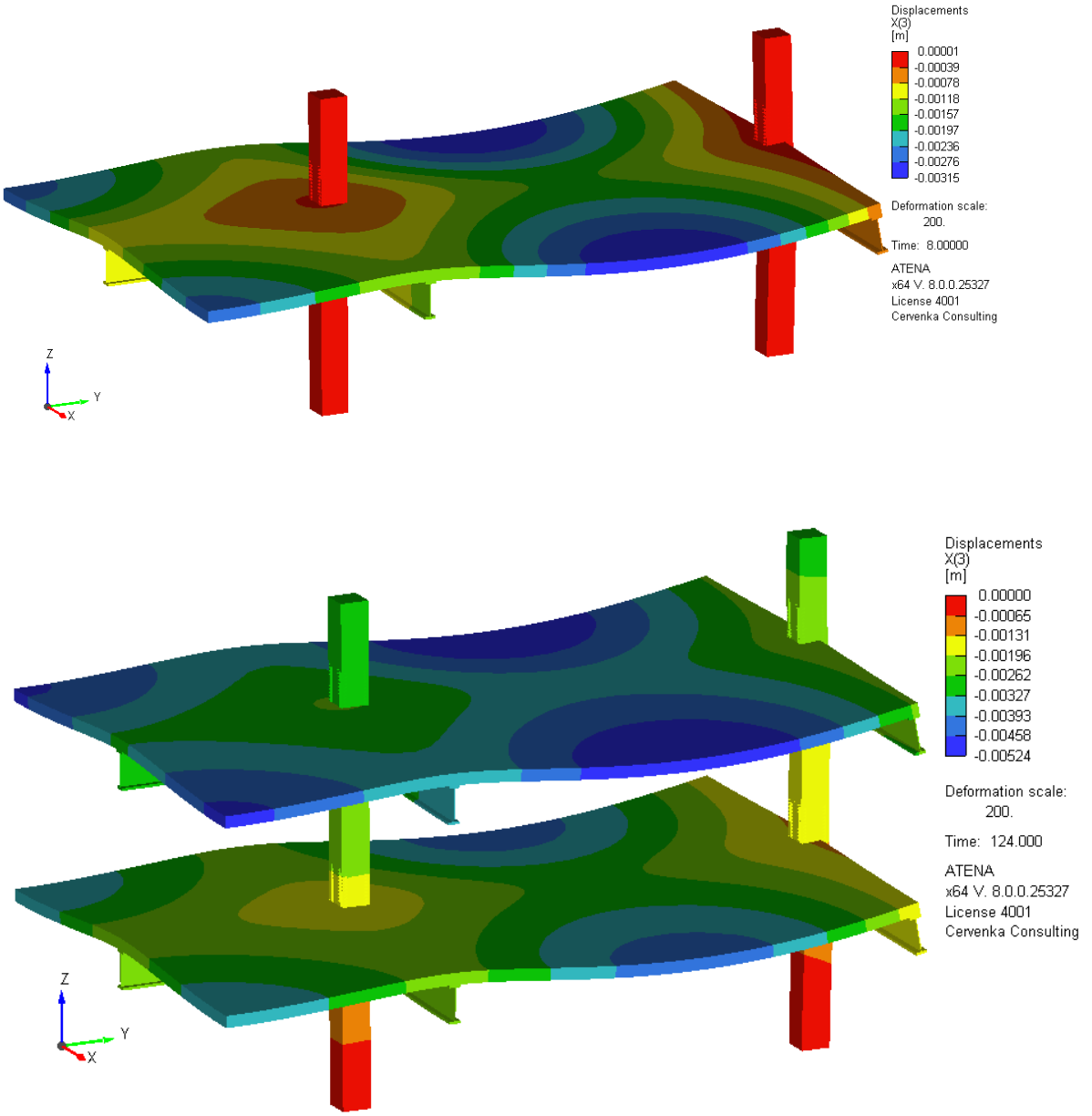

Fig. 43: Vertical deflections and modelling of the construction process in ATENA – CeSTaR-3 Green Concrete module.

The final checks of the structural behavior at the early stages should involve checking the level of concrete stresses (see Fig. 44). It should be noted that higher stress than the current concrete strength can be observed due to stress localization namely in the sharp corner between concrete and steel elements. However, the concrete should not reach the crushing state, which in ATENA software can be documented by the softening flag in the Yield/Crush Info – Softening flag as shown in Fig. 45.

Another important quantity to check is the cracking in concrete during the construction. The crack widths should be limited to micro-cracks that are barely visible. Crack widths and cracking pattern for the selected material PFA30 are shown in Fig. 31. It demonstrates that the crack widths

are around 0.02 mm. The visibility crack limit is 0.05 mm and the typical crack limit in concrete design is 0.3 mm. The concrete cracking is satisfying both these limits.

The other quantities that should be checked are stresses in the steel members of the MRCS connection as well as the stresses in the reinforcement. In this case, they are clearly below the yielding strength of the steel σ_y = 200 MPa and f_{sy} = 500 MPa for reinforcement.

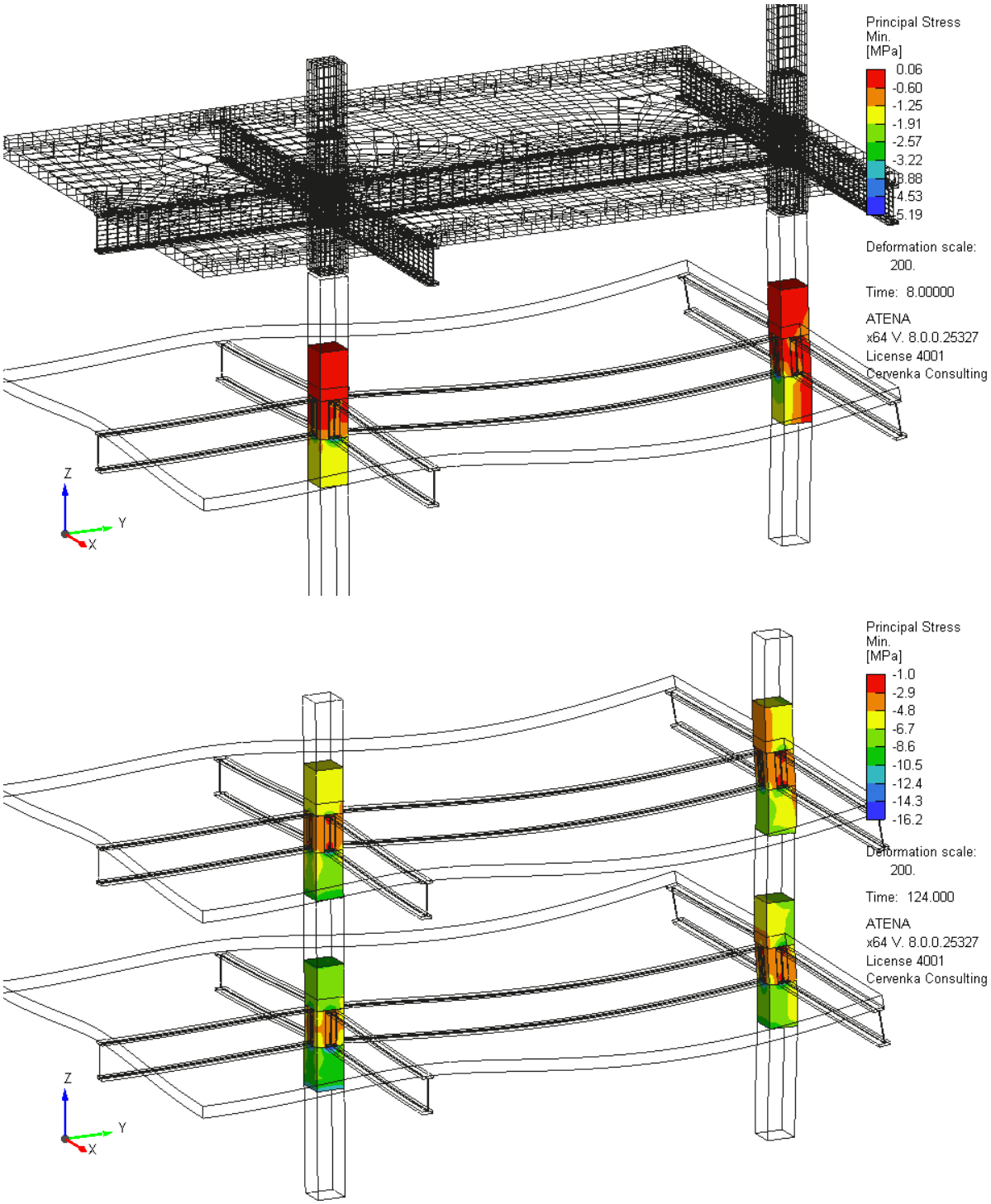

Fig. 44: Evolution of maximal concrete compressive stresses in the MRCS connection for frame example with PFA30 material. The wire frame in the top figure indicates the part of the model, which is not yet activated/constructed.

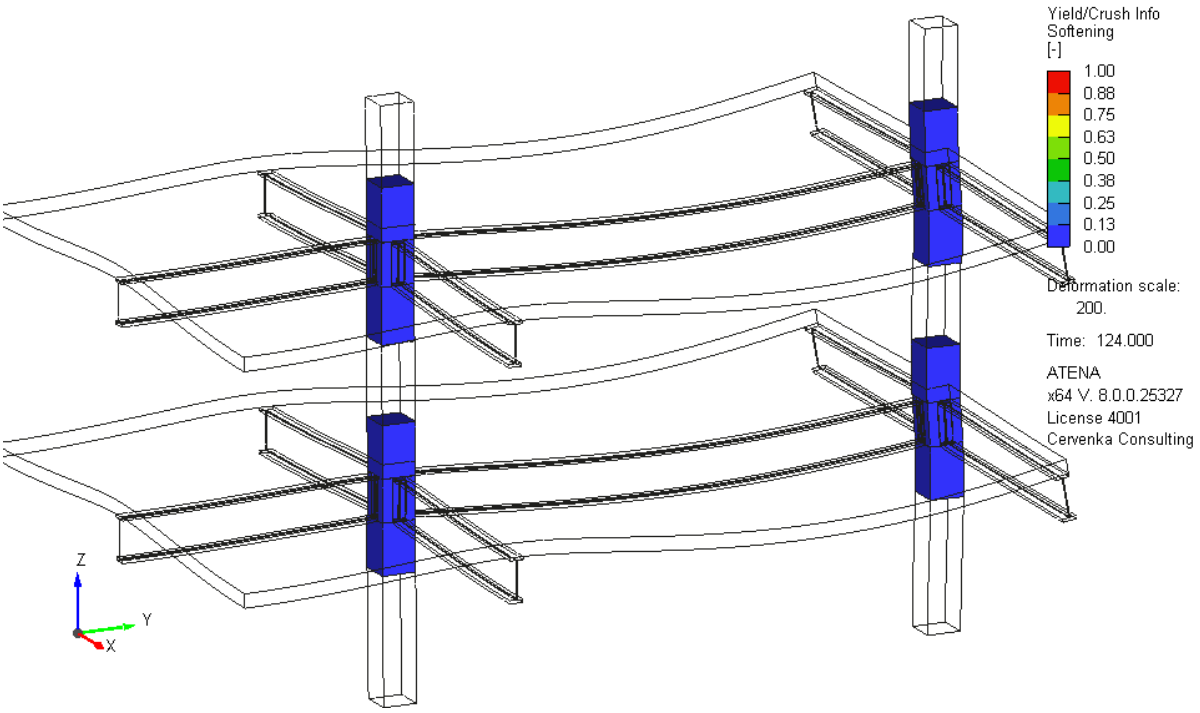

Fig. 45: Proof of no concrete crushing during the construction of MRCS frame example with PFA30 material.

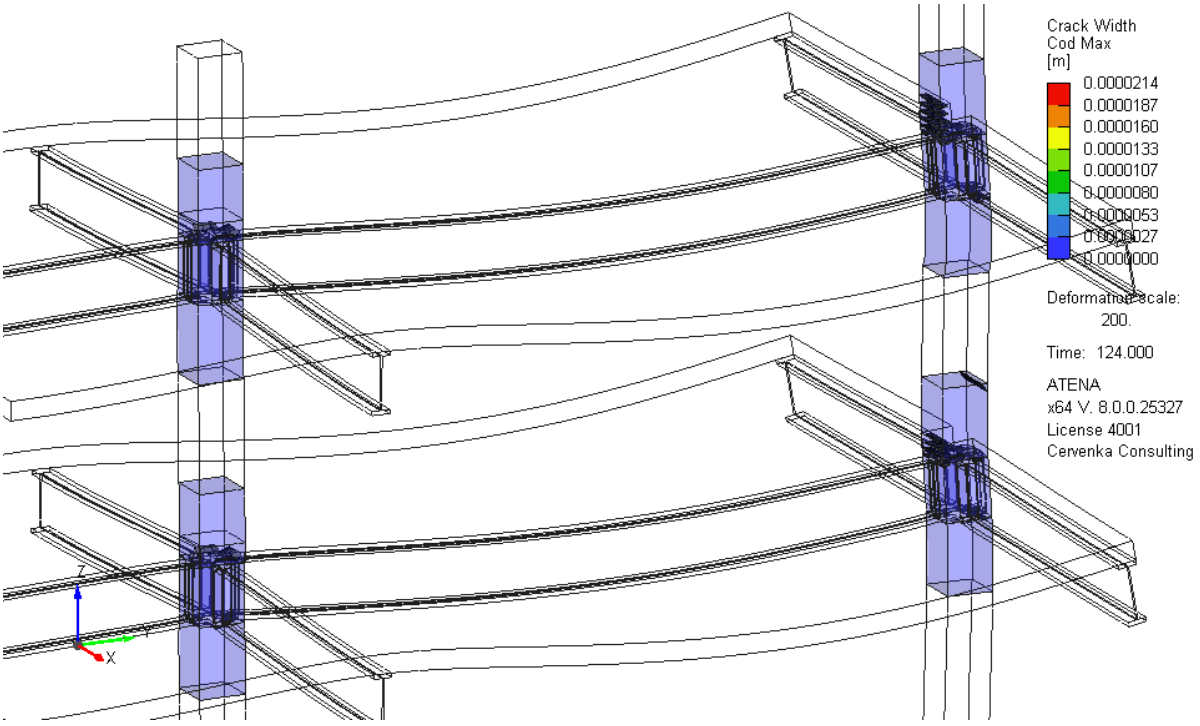

Fig. 46: Cracking at the end of the simulated construction sequence for MRCS frame example for material PFA30.

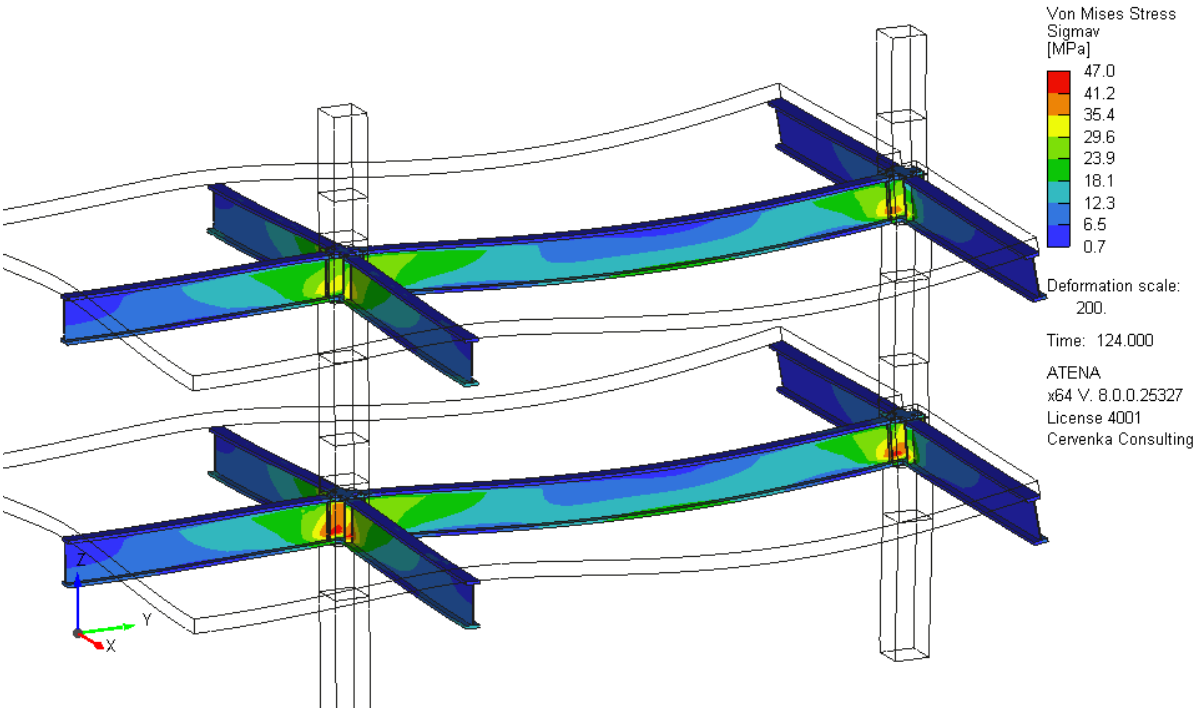

Fig. 47: Steel member stresses at the end of the simulated construction sequence for MRCS frame example for material PFA30.

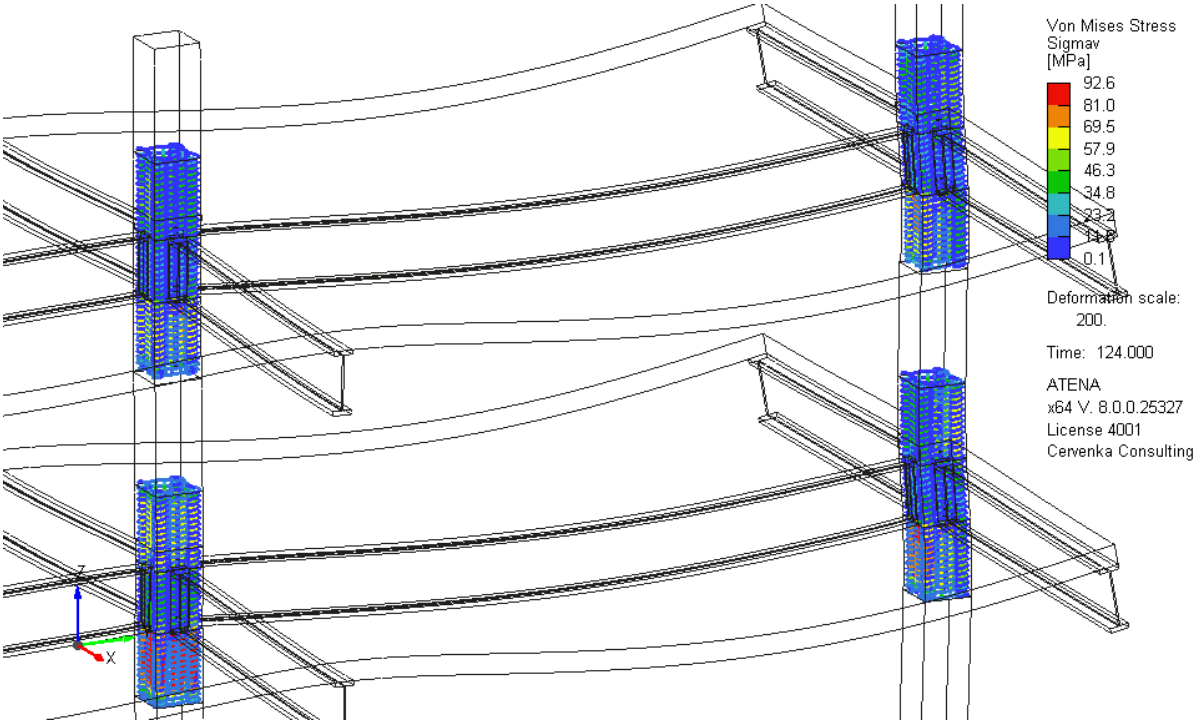

Fig. 48: Fig. 49: Steel member stresses at the end of the simulated construction sequence for MRCS frame example for material PFA30.

6 Conclusion

This document has presented a **design and optimization methodology for prefabricated structural systems made of green concrete with increased content of supplementary cementitious materials (SCMs)**, developed within the CeSTaR-3 project as result **TM04000013-V5**. The methodology addresses key challenges associated with the application of green concrete in practice, in particular the **time-dependent development of material properties** and its interaction with **staged construction and loading processes** typical for prefabricated systems.

The proposed approach is based on a **structured design framework** combining experimental knowledge, maturity-based material characterization, and numerical simulation. Central to the methodology is the explicit evaluation of structural response throughout the construction sequence, formulated in a standard **action–resistance format** consistent with Eurocode and fib Model Code principles. This enables rational assessment of safety and utilisation at critical construction stages rather than relying on conservative assumptions based on a single reference age of concrete.

By integrating experimentally derived material maturity curves with staged nonlinear analysis, the methodology provides a practical basis for **selecting suitable green concrete mixtures and optimising construction sequences**. The approach supports informed design decisions that balance structural safety, material efficiency, and construction feasibility, and allows the effective use of green concrete materials with slower early-age strength development.

The methodology is applicable to a broad class of **New-MRCS and related prefabricated concrete–steel structural systems**, but its principles can also be extended to other prefabricated or staged construction scenarios involving time-dependent concrete behaviour. Numerical simulation is employed as a **design support and verification tool**, ensuring transparency, traceability, and consistency of the design process.

Overall, the Green Concrete Design and Optimization Methodology provides a **practically applicable and performance-oriented framework** for the adoption of low-carbon concrete technologies in structural engineering practice. By enabling the safe and efficient use of green concrete in prefabricated systems, the methodology contributes to the broader objective of **sustainable and resource-efficient construction**.

7 References

[1] Argyris JH. 1954 Energy Theorems and Structural Analysis. Aircraft Engineering and Aerospace Technology. Emerald, 1954.

[2] Benes S., Mikolášková J., Altman T., 2025. ATENA Program Documentation, User's Manual for ATENA Studio, Cervenka Consulting s.r.o., www.cervenka.cz

[3] Bentz, E.C., Vecchio, F.J., Collins, M.P. 2006. Simplified Modified Compression Field Theory for Calculating Shear Strength of Reinforced Concrete Elements. ACI Material Journal, Jul/Aug 2006.

[4] Castaldo, P., Gino, D., Bertagnoli, G., Mancini, G. 2018. Partial safety factor for resistance model uncertainties in 2D non-linear analysis of reinforced concrete structures, Engineering Structures, 176, 746-762. https://doi.org/10.1016/j.engstruct.2018.09.041.

[5] Castaldo, P., Gino, D., Bertagnoli, G., Mancini, G. 2020. Resistance model uncertainty in non-linear finite element analyses of cyclically loaded reinforced concrete systems, Engineering Structures, 211(2020), 110496, https://doi.org/10.1016/j.engstruct.2020.110496

[6] Cervenka, V., Gerstle, K., 1971. Inelastic analysis of reinforced concrete panels. Part I , Theory. Part II, Experimental verification and Application. Publication IABSE 31 (11), 32-45.

[7] Cervenka, V., 1985, Constitutive Model for Cracked Reinforced Concrete. ACI Journal Nov.-Dec. 1985, 877-882.

[8] Cervenka, V., Margoldova, J. 1995, Tension Stiffening Effect in Smeared Crack Model, Engineering Mechanics, Stain Sture (Eds), Proc. 10th Conf., ASCE EMD, May 21-24, 1995, Boulder, Colorado, pp. 655-658

[9] Cervenka, J, Bittner, Z, Havlasek, P, Rehounek, L, GREEN CONCRETE PRE-CAST ELEMENTS DESIGN AND OPTIMIZATION, Project Result TM04000013-V5, Cervenka Consulting s.r.o., 2025

[10] Cervenka J, Cervenka V, Eligehausen R, 1998 Fracture-plastic material model for concrete. Application to analysis of powder actuated anchors, FraMCoS 3, Gifu, Japan, eds. H. Mihashi and K. Rokugo, Aedificatio Publishers, Freiburg, Germany, Vol. 2, pp. 1107-1116.

[11] Cervenka J. & Papanikolaou V. 2008. Three Dimensional Combined Fracture-Plastic Material Model for Concrete. *Int Journal of Plasticity*. 24:2192-2220. doi:10.1016/j.ijplas.2008.01.004

[12] Cervenka, J., Cervenka, V., Laserna S., 2014, On finite element modelling of compressive failure in brittle materials, Computational Modeling of Concrete Structures. Bicanic et al.(Eds),Euro-C 2014, St. Anton

[13] Cervenka, J., Cervenka, V., Laserna. S., 2018a. On crack band model in finite element analysis of concrete fracture in engineering practice, Engineering Fracture Mechanics, Volume 197, 2018, Pages 27-47, ISSN 0013-7944, https://doi.org/10.1016/j.engfracmech.2018.04.010.

[14] Cervenka V. Global safety format for nonlinear calculation of reinforced concrete. Beton- und Stahlbetonbau, 103, special edition. Berlin: Ernst & Sohn; 2008. p. 37–42.

[15] Cervenka V. Reliability-based non-linear analysis according to model code 2010. J fib Struct Concr. 2013;14(1):19–28.

[16] Cervenka V, Cervenka J, Kadlec L. 2018b. Model uncertainties in numerical simulations of reinforced concrete structures. Structural Concrete; 2018: 2004–2016. https://doi.org/10.1002/suco.201700287

[17] Cervenka, V., Cervenka, J., Jendele, L., 2025. ATENA Program Documentation, Part 1: Theory, Cervenka Consulting s.r.o., www.cervenka.cz

[18] Cervenka, V., Rimkus, A., Gribniak, V., Cervenka, J., 2022. Simulation of the Crack Width in Reinforced Concrete Beams Based on Concrete Fracture. Theoretical and Applied Fracture Mechanics, 121 (2022) 103428. https://doi.org/10.1016/j.tafmec.2022.103428

[19] Cervenka, V., Cervenka, J., Rymes, J., Numerical simulation of concrete structures-From research to engineering application, Structural Concrete. 2024;1–22., 2024 fib. International Federation for Structural Concrete, DOI: 10.1002/suco.202300016

[20] Cervenka, J., Zenisek, M., Altman, T., ATENA MODULE FOR NEW MULTI-SPIRAL REINFORCED CONCRETE AND STEEL COLUMN-BEAM CONNECTIONS, Project Result TM04000013-V1, Software Documentation, Cervenka Consulting s.r.o., 2025
[21] Cervenka, J., Zenisek, M., Altman, T., ATENA MODULE FOR GREEN CONCRETE MODELLING AND DESIGN, Project Result TM04000013-V2, Software Documentation, Cervenka Consulting s.r.o., 2025
[22] Engen M, Hendriks M., Köhler J, Overli JA, Aldtstedt E. 2017. A quantification of modelling uncertainty for non-linear finite element analysis of large concrete structures. Structural Safety 2017; 64: 1-8.
[23] EN 1990, 2023. Eurocode 0: Basis of structural design. European Committee for Standardization (CEN). Brussels.
[24] EN 1992-1-1, 2022. Eurocode 2: Design of Concrete Structures - Part 1-1: General ruels and rules for buildings. European Committee for Standardization (CEN). Brussels.
[25] *fib* MC 2010 . International Federation for Structural Concrete. Model Code for Concrete Structures 2020. Berlin: Wilhelm Ernst & Sohn; 2013.
[26] *fib* MC 2020, Model Code for Concrete Structures 2020. Bulletin 105, International Federation for Structural Concrete (2022).
[27] Gino D, Castaldo P, Giordano L, Mancini G. 2021. Model uncertainty in nonlinear numerical analyses of slender reinforced concrete members. Structural Concrete. 1–26. https://doi.org/10.1002/suco.202000600
[28] Grassl, P, Xenos, D, Nyström, U, Rempling, R, Gylltoft, K: CDPM2: A damage-plasticity approach to modelling the failure of concrete. International Journal of Solids and Structures, 50(24) (2013).
[29] Harries, K. A., Kharel, G.: Experimental investigation of the behavior of variably confined concrete. Cement and Concrete Research, 33 (2003).
[30] Havlásek, P.: Numerical modeling of axially compressed circular concrete columns. Engineering Structures, 227 (2021).
[31] Jirásek, M., Bažant, Z.P. 2001. Inelastic Analysis of Structures, John Willey & Sons, LTD, Baffins Lane, Chichester, England, ISBN 0-471-98716-6
[32] Joju, J. Development of Composite Beam-Column Joints for New RCS Systems. Ph.D Thesis, National Taiwan University, Taiwan, China, 2024.
[33] Joju, J., Ou, YC. (2025). Development of High-Strength Reinforced Concrete Column and Steel Beam (New-RCS) Structural System. In: Yang, J., Fu, J., Liu, A., Ng, CT. (eds) Proceedings of the First International Conference on Engineering Structures. ICES 2024. Lecture Notes in Civil Engineering, vol 599. Springer, Singapore. https://doi.org/10.1007/978-981-96-4698-2_33
[34] Jones Joju, Yu-Chen Ou, Chia-Chi Chang, Influence of axial compression on the bearing behavior of high-strength reinforced concrete column and steel beam (New-RCS) joint, Engineering Structures, Volume 345, Part A, 2025, ISSN 0141-0296, https://doi.org/10.1016/j.engstruct.2025.121447.
[35] Jones Joju, Yu-Chen Ou, Hsiang-Chih Tsai, Jui-Chen Wang, Seismic performance of through-column beam-column joints for composite reinforced concrete-steel (RCS) frames with circular high-strength columns, Engineering Structures, Volume 342, 2025,ISSN 0141-0296, https://doi.org/10.1016/j.engstruct.2025.120884.
[36] Kučerová, A., Sýkora. J, Havlásek, P, Jarušková, D, Jirásek, M.: Efficient probabilistic multi-fidelity calibration of a damage-plastic model for confined concrete. Computer Methods in Applied Mechanics and Engineering, 412 (2023)
[37] Li, P, Wu, Y.-F.: Stress–strain behavior of actively and passively confined concrete under cyclic axial load. Composite Structures, 149 (2016).
[38] Menétrey, P., Willam, K.J. 1995. Triaxial failure criterion for concrete and its generalization. ACI Structural Journal 92 (3), 311-318.

[39] Ngo, D., Scordelis, A.C. 1967. Finite element analysis of reinforced concrete beams, J. Amer. Concr. Inst. 64, pp. 152-163.
[40] Patzák, B.: OOFEM - an object-oriented simulation tool for multi-physics problems. Acta Polytechnica, 52(4) (2012).
[41] Rashid, Y.R. 1968. Analysis of prestressed concrete pressure vessels. Nuclear Engineering and Design 7 (4), 334-344.
[42] Rehounek, L., Zenisek, M., Numerical Simulation and Model Validation of Multispiral-Reinforced Concrete Columns' Response to Cyclic Loading, Buildings 2025, 15(21), 3855; https://doi.org/10.3390/buildings15213855
[43] Suidan, M., Schnobrich, W.C. 1973. Finite Element Analysis of Reinforced Concrete, ASCE, J. of Struct. Div., Vol. 99, No. ST10, pp. 2108-2121
[44] Turner M., Clough RW. 1956 Stiffness and deflection analysis of complex structures. Journal of the Aeronautical Science. Vol.23, September 1956, No. 9.
[45] [UV 39098, 2025] Utility model number 39098 - Mold for the production of test specimens, The Industrial Property Office of the Czech Republic, 19. 12. 2025.
[46] Yu-Chen Ou, Jones Joju, Wei-Lun Wang, Composite RCS joint designs for circular high-strength reinforced concrete columns, Journal of Building Engineering, Volume 104, 2025, ISSN 2352-7102, https://doi.org/10.1016/j.jobe.2025.112233.
[47] Zienkiewicz O.C., Cheung Y.K. 1967. The Finite Element Method in Structural and Continuum Mechanics. McGraw-Hill, London, 1967. p 274.
[48] Zienkiewicz O.C., Valliappan S., King I.P. 1969. Elasto-plastic solutions of engineering problems 'initial stress' finite element approach. Int. Journal for Numerical Methods in Engineering. Volume1, Issue1, January/March 1969, pp. 75-100 https://doi.org/10.1002/nme.1620010107